Low Molecular Mass Gelators of Organic Liquids and the Properties of Their Gels

Pierre Terech*,† and Richard G. Weiss‡

Laboratoire Physico-Chimie Moléculaire, UMR 585, Département de Recherche Fondamentale sur la Matière Condensée, C.E.A.-Grenoble, 17, Rue des Martyrs, 38054 Grenoble Cédex 09, France, and Department of Chemistry, Georgetown University, Washington, DC 20057-1227

Received March 10, 1997 (Revised Manuscript Received July 2, 1997)

Contents

I. Introduction

This review explores the properties of thermally-reversible viscoelastic liquidlike or solidlike materials (i.e., *organogels*) comprised of an organic liquid and low concentrations (typically <2 wt %) of relatively low molecular mass molecules (i.e., *gelators*). The physical characteristics of organogels can range from those of surfactants in solution[1] (e.g., micellization, lyotropism, and crystallization) to those of polymer solutions[2] (e.g., swelling and microscopic mass motion); gels are at the interface between "complex fluids"[3] and phase-separated states of matter. Some of the important physical properties of organogels, the techniques used to probe their properties and structures, and the basic thermodynamic concepts involved in gelator aggregation in organic liquids will be discussed.

As noted prophetically by Dr. Dorothy Jordon Lloyd nearly 70 years ago, "....the colloid condition, the gel, is easier to recognize than to define".[4] This and other empirical definitions of the gelled state, including the first by Thomas Graham in 1861,[5] relied on the qualitative macroscopic observations that were available. The first attempt to link macroscopic and microscopic properties to define a gel was made by Hermans.[6] It served as the basis for what is, perhaps, the most comprehensive (and cumbersome to apply!) definition advanced more than 20 years ago by Flory.[7] Thus, a substance is a gel if it (1) has a continuous structure with macroscopic dimensions that is permanent on the time scale of an analytical experiment and (2) is solidlike in its rheological behavior. For screening purposes, the dictum of Jordon Lloyd is still useful and preferred by at least one of the authors: if it looks like "Jello", it must be a gel!

An organogel is usually prepared by warming a gelator in an organic liquid until the solid dissolves, and then cooling the solution (or sol) to below the gelation transition temperature (i.e., the temperature below which flow no longer is discernible over long periods). The resulting material is a gel or jelly depending upon its hardening or thickening ability; the formal description and classification is based upon rheological properties. Colloidal aggregates (i.e., whose typical dimensions fall between 20 and 2000 Å) in the gel are linked in complex, three-dimensional networks that immobilize the liquid component to a variable extent (principally) by surface tension.

In spite of the many chemical compositions and physical properties of gels that are known, several important questions remain to be answered. Among these are:

(1) What are the structural requirements for a molecule to gel an organic liquid?

(2) What is the relationship (if any) between the packing arrangements of gelator molecules in their *bulk* crystalline states and in their various aggregates in the gels?

(3) How does the molecular packing of gelator molecules in their aggregates influence the mechanical, thermodynamic, optical, and other properties of the gels?

These and other basic questions relate to a practical goal—to discern *a priori* whether and under what conditions an organogel will form. In this context, representative groups of low molecular mass molecules known to gel organic liquids and some examples of their gels are examined. When possible, correlations are made among the structures and electronic properties of the gelators, the liquids, and the phenomenological and physical properties of their gels.

---

† Address correspondence to this author at Laboratoire Physico-Chimie Moléculaire. Member of C.N.R.S.
‡ Georgetown University.

S0009-2665(97)00028-9 CCC: $28.00 © 1997 American Chemical Society

Pierre Terech received his Diplome d'Ingénieur in 1976 from the Ecole Nationale Supérieure de Chimie de Paris, France. He joined the Commissariat à l'Energie Atomique (CEA) in Grenoble, France, and the laboratory of Professor A. Rassat to defend in 1979 a thesis on the use of electron paramagnetic resonance spectroscopy to investigate electron charge transfer in donor–acceptor complexes. In 1983, he received his Doctorat d'Etat in Physics (structural studies of gels) under the mentorship of Professors A. Rassat and F. Volino. He is a member of the Centre National de la Recherche Scientifique (CNRS) since 1983. He received two National Awards in 1984, from the Société Française de Physique and Société Française de Chimie. He spent 1 year in a research center of the French oil company Elf Aquitaine, working to improve the performance of lubricating greases. From 1986 to 1992, he was a staff physicist in charge of small-angle scattering spectrometers at the European neutron source, ILL, Grenoble. He spent a part of 1992 as a guest G. B. McKenna (NIST, Gaithersburg, MD), studying the structural and mechanical properties of gelling and polymeric membrane systems. In 1993, he returned to CEA, Grenoble, where he is presently head of a research laboratory in a CEA–CNRS–University of Grenoble collaborative unit. His current experimental efforts are directed toward the understanding of aggregation phenomena in complex viscoelastic systems, such as colloids, gels, and composites.

Richard G. Weiss was born in Akron, OH, on (Friday) November 13, 1942. He received an Sc.B. degree in chemistry from Brown University in 1965, an M.S. (1967) and a Ph.D. (1969) degree from the University of Connecticut under the mentorship of Eugene I. Snyder and spent two years on an NIH Postdoctoral Fellowship at California Institute of Technology with George S. Hammond. In 1974, after three years as Visiting Assistant Professor (and NAS Overseas Fellow) at the Instituto de Quimica of the Universidade de São Paulo in Brazil, he joined Georgetown University where he is currently Professor of Chemistry. His research interests include reactions in constrained environments, photochemistry, design and transformation of liquid crystals and other molecular assemblies, the modification and microscopic investigation of polymers, and ...gels (edible or otherwise).

The most "efficient" mode for the immobilization of a large volume of liquid by a small quantity of gelator is for the elementary assemblies to be rodlike. The structure of linear aggregates in the gel is determined by the direction and strength of the binding forces associated with the aggregation process. In aqueous solutions of amphiphiles, aggregate structures result from a balance between the attractive (interfacial) and repulsive forces (between head groups).[8]

Since hydrophobic attractions, a major driving force for aggregation in water,[8] are either not operative or of secondary importance in many organic liquids, aggregation in organogels must result from a different set of interactions.[9−11] In nonaqueous liquids, the attractive forces are mainly dipolar interactions and, possibly, specific intermolecular hydrogen bonds or metal-coordination bonds. They must balance the free energy increase that accompanies reductions in translational and rotational freedom of motion.

Aggregation of surfactants in organic liquids[12] has been the subject of theoretical and quantitative treatments.[13] Usually, beyond a concentration threshold (C_{mic}) that is normally much less pronounced than the analogous critical micellar concentration (CMC) of aqueous systems, finite spherical micelles are formed. By contrast, when a small amphiphilic molecule is a gelator and/or when its concentration is properly adjusted, the formation of colloidal aggregates can be observed.

As long as only the topology of the aggregates is considered and compared to various simple geometries (e.g., spheres, lamellae, and fibrils), characteristics of the rodlike structures can be related to the thermodynamics of the suspensions. At equilibrium, the optimal configuration is obtained by considering the influence of both the ratio of the cross-sectional areas of a hydrocarbon chain and polar moieties of the gelator and the polarity of the solvent on free energy. Depending on the excess of free energy corresponding to the hemispherical caps of the chain extremities, either "infinitely long" giant micelles or numerous shorter ones (the entropically favored case) are formed.

Aggregation can be due to hydrogen-bonding, organometallic coordination bonding, electron transfer, etc. between gelator molecules, with a strength function (ψ) that depends on the intermolecular interaction energy (αkT). In turn, α is directly related to the number and type of intermolecular interactions per gelator molecule and the number of gelators within a cross-sectional area of an aggregate. The simplest case is for molecular threads with only one gelator molecule per cross-sectional repetition unit and only one principal type of intermolecular interaction. The gelator−gelator interaction energy determines the aggregation threshold ($C_{cri} \propto e^{-\psi(\alpha)}$) and the size distribution of the aggregates. The size distribution of the chainlike aggregates, correlated to the contour length (L) and flexibility ($\langle l_p \rangle$), is usually very broad and depends strongly on gelator concentration and temperature. It can also depend on the (very small) concentration and structure of cosurfactants that have a strong affinity for the gelator and function as "chain terminators" or "chain-growth inhibitors" by interrupting gelator−gelator interactions.

Growing rodlike aggregates engage in dynamic exchange of gelator molecules with the surrounding bulk liquid. The size distribution of the aggregates results from a combination of the entropic decrease on aggregation and standard free energy variation between the nonaggregated and the aggregated states of the surfactant. In organogels, this condition does not apply and infinite, fiberlike aggregates are formed while *normal* phase separation into macroscopically separated crystalline and liquid layers is avoided due to the existence of both an interconnected, solidlike, three-dimensional (3D) gelator organization and a balance of opposing forces related to aggregate interactions. The required balance contributes to the relative rarity of these systems.

Unlike some aqueous two-component systems,[14] sphere-to-rod phase transitions are usually not well-characterized in binary organogelator systems. In spite of broad distributions of aggregate lengths, cross-sectional dimensions can be rather monodisperse (see below). When the gelator concentration is increased to the overlap value (C^*, in analogy with polymeric solutions), chains are no longer separated (as in the "dilute" concentration regime), their rotation becomes hindered, and the equivalent spherical volumes of the linear aggregates overlap. A network with an average mesh size (ξ) is formed.

Surfactant organogels can exhibit either permanent rigid networks or transient semiflexible meshes. The notion of transient mesh size or statistical porosity of a 3D network is similar to the description of polymeric solutions (with "blobs" of size ξ) when individual chains interact with each other.[2] In essence, gelation occurs when normal crystallization has gone awry. Instead of the solid component separating in crystals, the ratio of whose dimensions is almost invariant with overall size, fibers are formed in which the cross-sectional dimensions are nearly constant irrespective of the overall aggregate length.

Examples treated here are primarily in the semidilute concentration range, corresponding to overlapped chainlike aggregates (isotropic gels) with a cursory examination of the concentrated range, where chains are somewhat ordered (anisotropic gels).

Factors affecting the aggregation process are relevant for describing the gelation phenomenon. They include the solvent nature, the polarity, conformational lability, and molecular shape of the gelator, the temperature, and the possible participation of cosurfactants. Some structural and kinetic aspects of the aggregation/gelation process are also consistent with its being viewed as a phase separation involving a nucleation reaction, thus emphasizing the role of the interfacial free energy of the gelators (in contrast to spinodal decomposition phenomena or unwinding processes).

Since cosurfactants can influence strongly the types of aggregates and phases, the composition and the method of preparation of the gelling mixtures must be controlled carefully. In particular, comicellization may shift the cooperative aggregation process to concentrations higher than the true C_{mic} and/or initiate a sphere-to-rod transition necessary for gelation of the mixture at C^*. Above C^*, individual aggregates of a sol-phase (i.e., a collection of finite aggregates in a liquid solution) are interconnected in an infinite 3D superaggregate or network.

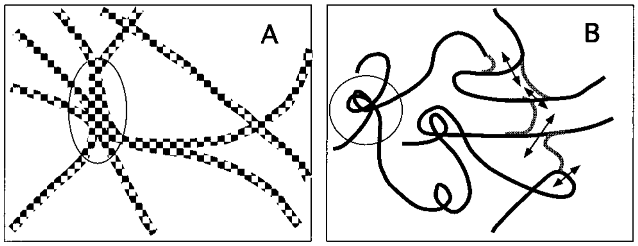

Figure 1. Physical properties of organogels are dependent upon the nature of their networks. (A) "strong" gels with permanent solidlike networks in which the nodes are spatially extended (pseudo)crystalline microdomains. (B) "weak" gels with transient networks exhibiting no elasticity over long time periods in which the nodes are entanglements or spatially limited organized microdomains. Additional kinetic features such as chain breaking/recombination (arrows) may occur as in the case of "living polymers".

The macroscopic recognition of a gel state is somewhat ambiguous, and various classifications have been proposed based on either morphology, consistency, or chemical and mechanistic considerations.[15-17] Rheological properties appear to be the best diagnostics to follow the changes in gelator aggregation during the sol-to-gel and gel-to-sol (melting) phase transitions.[18] They can be described by statistical physics, and, in particular, percolation models[19,20] can simulate the mechanical behavior near the critical gelation threshold. The sol-to-gel phase transition is generally characterized by a divergence of the connectivity correlation length[21] (as is the case for second-order phase transitions).

As mentioned, two different types of 3D networks and viscoelastic materials can be obtained in organogel systems (Figure 1). In the first, materials exhibiting a solidlike, viscoelastic, mechanical behavior and which are made of permanent networks obtained through a sharp solution- or sol-to-gel phase transition at a specific temperature (T_{SG}) are "strong" gellike systems. In the second, materials exhibiting a liquidlike viscoelastic behavior which are made of transient networks (obtained through a much smoother threshold somewhat analogous to the glass transition of polymers) are termed "weak" gellike systems. They usually exhibit enhanced elasticity on short time scales. Both types of networks are thermally reversible. On heating, the supramolecular architecture is melted and individual molecules (or separated strands of aggregated molecules) are redispersed in the bulk solution. The static and dynamic quantities of some "weak" gel systems follow power laws which can be approached by incorporating the concentration and temperature dependencies of the length of the strand assemblies in the scaling laws for semidilute polymers in good solvents (as with "living polymers").

Depending upon the balance between attractive and repulsive forces, various lyotropic organizations can be observed when the gelator concentration is $>>$ C^*. Bulk phases or microdomains in the heterogeneous network can produce nematic, hexagonal, or rectangular orderings.

II. Techniques

An efficient methodology to elucidate the nature of an organogel is to begin with a characterization of its rheological and thermodynamic properties. Rheology offers a convenient method to measure the flow properties of gellike materials and facilitates the classification between "strong" and "weak" gel types.[15] Strictly speaking, "weak" gels (or viscoelastic liquids) do not fulfill the mechanical requirements of a *true* gel.[18] Since their flow properties depend upon gelator concentration and angular frequency (ω) of the applied stress, they are included in discussions here. Mechanical parameters indicate the natures of the aggregate networks which, in turn, suggest the nature of the interactions responsible for their cohesion. Procedures such as steady shear, oscillation, stress relaxation, and creep experiments can probe the mechanical properties of the soft viscoelastic materials. The elastic and viscous components, mixed in such non-Newtonian materials, are measured in oscillatory experiments in which a small periodic strain/stress is applied within the appropriate amplitude range defining the linear regime. For solidlike gels, the elasticity measured by the storage modulus $G'(\omega)$ is much larger than the dissipated energy (or viscous behavior as measured by $G''(\omega)$) and extends as a plateau from short to long times.[18] These systems are characterized by a yield value (σ^*) at typical time scales of seconds or hours and which is the minimum stress that causes flow to occur. Frequently, comparisons and analogies between the structural and mechanical properties of organogels and thermoreversible networks of some aqueous biopolymer gels[22−24] can be made since the gel state is frequently involved in natural materials.

After elucidation of the basic mechanical features, characterization of the phase diagram and determination of the sol-to-gel phase transition temperature (T_{SG}) are necessary. The methods used for this purpose include differential scanning calorimetry (DSC), temperature sweep rheological experiments, and different spectroscopies (fluorescence, IR, EPR, NMR, etc.) using the amplitude variation of a spectral feature with temperature to trace the aggregation phenomenon (during which gelation occurs). The melting process of physical gels at a temperature (T_{GS}) can be analyzed in a simplified framework already utilized with gelatin gels.[25] The related model assumes that the network cohesion comes from cross-links resulting from binary associations of macromolecular chains. A combination of the mass-action constant, van't Hoff's law, and various simplifying hypotheses leads to eq 1, which relates the

$$\ln C = -\Delta H°/RT_{\mathrm{GS}} + \text{constant} \qquad (1)$$

exothermic heat of association ($\Delta H°$) to T_{GS}. An approach considering the melting of the gels as a dissolution process of crystals according to the Schröder−van Laar equation[26] leads to similar trends.[27]

The temperatures of the gel transitions are dependent on the physical techniques used to measure them. In addition, the T_{SG} from cooling and the T_{GS} from heating samples usually differ due to hysteresis effects, regardless of the technique of measurement. Temperatures based on rheological experiments are most accurate, since, microscopically, they report the point at which colloidal contacts and/or colloidal structures themselves are interrupted (for T_{GS}) and, thus, when flow begins, or when colloids of strands enter into semipermanent contact with each other throughout the sample (for T_{SG}). The values indicated by spectroscopic measurements can differ significantly from the rheological ones; the changes detected spectroscopically need not correlate with cessation or initiation of flow, since they measure microscopically structural modifications of strand organization within a colloid, the formation or dissolution of individual strands, etc. The difference between transition temperatures measured via rheology and spectroscopy is smallest when the change in gelator solubility with temperature is greatest.

Once the rheological and thermodynamic properties of an organogel have been explored, it is useful to investigate the structures of the unidirectional aggregates whose interactions are responsible for viscoelasticity. Electron micrographs are informative but should be combined with complementary methods, like scattering techniques. Electron microscopy (EM) provides structural information in direct space; scattering data are reported in reciprocal distance space, necessitating a mathematical analysis and transformation to extract structural information.

Samples for EM experiments are usually prepared by temperature quenching and subsequent fracture, etching, and metal shadowing steps. Direct imaging methods, originally used for biological systems,[28,29] are now used for analogous aqueous systems[30] and should be the method of choice with organic media to minimize perturbations. Even so, artifacts may arise if confinement of the gel in very thin layers distorts colloidal sizes or chain flexibilities and the topology of entanglements.

Scattering information on organogels can usually be obtained by using bulk samples that are unadulterated (except for deuteration of the liquid component when small angle neutron scattering (SANS) is the method of choice). SANS or small angle X-ray scattering (SAXS) data provide information on correlation distances typical of colloidal systems and can utilize some contrast variations.

Although the structural models deduced from the analyses of the scattering curves have no unique solution (due to the lack of phase information and spatial resolution), small-angle scattering (SAS) techniques (for instance SANS or SAXS) have been shown to be very reliable in characterizing colloidal aggregates.[31,32] For instance, calculation of the theoretical scattered intensity for rodlike scatterers which are uncorrelated in position and orientation simplifies under conditions of particle scattering[33,34] to a sum of the spherically averaged intensity for each long rod ($L >> 2r$; eq 2). C is the rod concentration

$$I = \frac{\pi C}{Q}\overline{\Delta b}^2 M_{\mathrm{L}}\left[2\frac{J_1(Qr)}{Qr}\right]^2 \qquad (2)$$

(g·cm^{-3}), M_L is the mass per unit length of rod (g·Å^{-1}), and $\overline{\Delta b}$ is its specific contrast (cm·g^{-1}). The momentum transfer Q (Å^{-1}) is defined as $Q = (4\pi/\lambda)$ sin θ, where θ is half the scattering angle. Use of appropriate Q-expansions of eq 2 can provide information concerning the directional anisotropy of the rodlike aggregates and structural features of their cross sections. Frequently, it is possible to identify in the experimental scattering curves the Q-domain of this form-factor.

A method that relates the morphs of a neat solid gelator and the molecular packing in gel strands has been developed.[35] The method involves a comparison of the powder diffraction patterns of the fibers in a gel (by subtraction of the large, broad diffraction of the (amorphous) liquid component from the pattern of the gel) and of the neat crystalline gelator (obtained from single crystal diffraction data). The two diffraction patterns are related if the molecular packing in the gelator is like that in the morph of the solved crystal.

An accurate structural and dynamical study of the aggregates in organogels may involve the determination of the length, flexibility, and diffusion coefficients of the chainlike aggregates. Within specific conditions, this can be achieved from elastic and quasi-elastic light scattering techniques.[36]

Additionally, molecular dynamics in thermoreversible networks can be investigated both “classically” with photon correlation spectroscopy[37] and with dielectric spectroscopy,[38] and further information on segmental motions of chainlike aggregates in gels can be gleaned from inelastic neutron scattering techniques, such as neutron spin echo spectroscopy.[39]

III. Classes of Organogelators

It is not yet possible to select *a priori* a molecule to gel definitively a selected liquid. Discoveries of new gelators or thickeners remain mainly fortuitous. As an aid to defining strategies for the molecular design of new low molecular-mass organogelators, many of the known ones have been grouped separately according to the subjective views of the authors.

A. Fatty Acid Derivatives

Substituted Fatty Acids and Monovalent Metal Salts. 12-Hydroxyoctadecanoic acid (**1**) and its related salts (**1$_M$**) are known to create hardened materials from organic liquids.[40,41] For decades, semisolid dispersions of **1$_{Li}$** in oils have been used in the lubrication industry.[42,43] In many ways, the historical application of techniques to study mixtures containing **1** is a prototype for the evolution of research in the field of low molecular mass gelators and their gels.

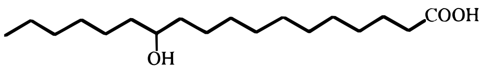

1

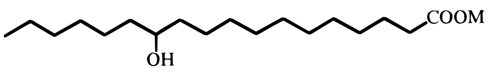

1$_M$

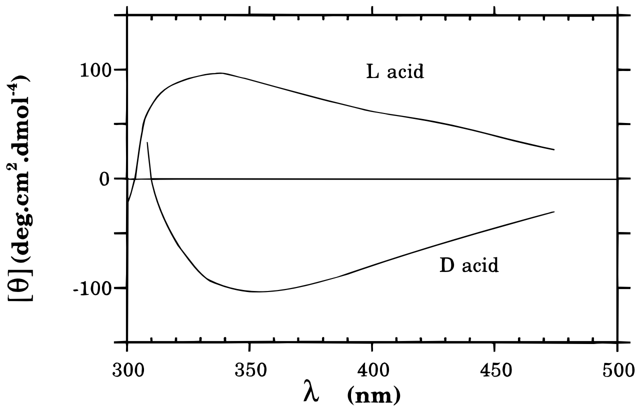

Figure 2. Enantiomeric CD bands of **1**/CCl_4 gels (10-mm thickness; 25.7 mmol·L^{-1} for the L acid, 35.7 mmol·L^{-1} for the D acid). The location of the CD maximum is dependent on the liquid. (Reprinted with permission from ref 50. Copyright 1979 Nature.)

The 3D networks of aggregated fatty acid molecules act as a “sponge”, maintaining the oil component in lubricating greases[43] close to the friction regions of metallic surfaces[44] in various mechanical systems. The dispersion process proceeds through lyotropic phase transitions[45] comparable in nature to the ability of some optically active acids to form lyotropic liquid crystals in organic solvents.[46] The first detailed study employed circular dichroism, X-ray diffraction, electron microscopy, differential scanning calorimetry (DSC), infrared spectroscopy (IR), and optical polarizing microscopy to characterize the different levels of organization of the colloidal materials.[47] Later, scattering techniques with powerful neutron and X-ray beams allowed an even more detailed structural investigation of gel aggregates whose sizes range from the microscopic (several angstroms) to the mesoscopic (several hundreds of angstroms).[48,49] The range of organic liquids which can be gelled by this family of molecules extends from alkanes, carbon tetrachloride (CCl_4), and aromatic solvents to more polar fluids, such as nitrobenzene. The kinetics of the sol-to-gel transition show that the onset of the elastic modulus is sharp. G' and G'' are virtually independent of frequency and the magnitude of G' is large ($G' = 3700$ Pa at $C \approx 0.35\%$). The physical junctions in the network appear as permanent cross-links at a given temperature in the gel domain of the phase diagram. Since **1** and **1$_M$** have an asymmetric carbon center, their aggregates can be chiral and have specific optical properties. The molecular packing in the strand aggregates of the gels differs from that found in the neat solid by limited gliding of special reticular planes. In general, *the molecular packing arrangements of gelators in gel strands and in neat crystalline phases should not be assumed to be the same*;[35] many gelators are polymorphous even as neat solids. There is a preferential reflection of circularly polarized light by the gels,[50] indicating that the fibers of **1** are twisted in a way that is related to their molecular chirality (Figure 2).

The observation of induced circular dichroism in achiral chromophoric molecules added to gels consisting of an achiral liquid and a chiral gelator confirms that the probes are intercalated into the supramolecular helical strands. Most of the helices are left-handed for the D-acid and right-handed for the L-acid. Observed superhelicities, whose origin is not

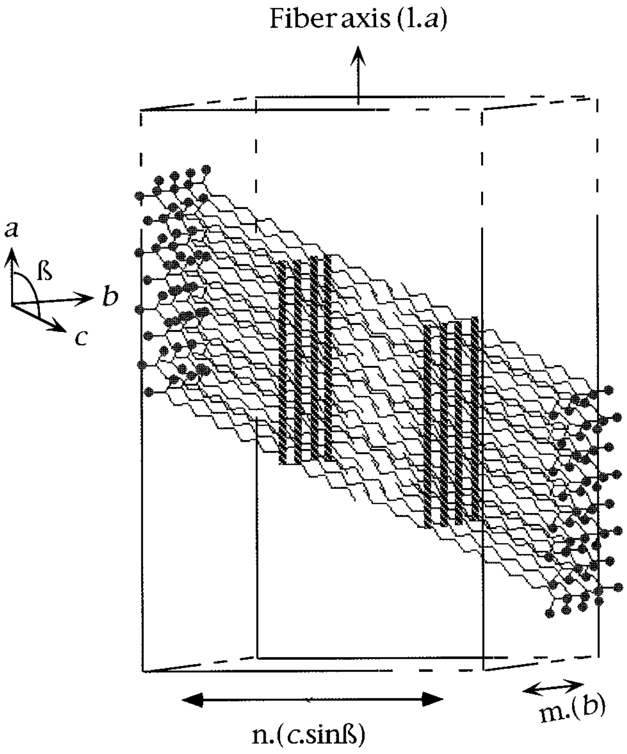

Figure 3. Structural model of fibrillar or ribbon-like aggregates of **1** as formed in gelled organic liquids. The crystallographic axis (monoclinic symmetry) and the fiber geometry are indicated. The dimensions are proportional to the crystallographic cell parameters, as shown. The thick lines represent H-bond sequences connecting the hydroxyl groups at C_{12} and the spheres are carboxylic end groups. (Reprinted with permission from ref 49. Copyright 1994 American Chemical Society.)

clearly established,[51] may result from a mechanically stressed chiral fiber during sample preparation. This phenomenon has been noted for some steroid-based organogelators[52] and for monolayers at the air−water interface.[53] Racemic (*d,l*)-**1** produces organogels consisting of fibers interconnected by plateletlike contact zones. Consequently, the enantiomorphic relationships do not fully explain the gelling ability in organic liquids.[49] By contrast, some aqueous chiral surfactant systems are observed to form fibers, while the racemic mixtures separate as plate-like crystals without any gel formation.[54,55] The topology of the cross sections of the rigid fibers is dependent upon the liquid type and varies from square in benzene (215 Å full side) to rectangular in nitrobenzene (ribbons of 300-Å width).[49] Due to the presence of carboxylic groups at the edges of the fibers, anisotropic lateral aggregation or growth of the fibers (which accounts for the development of "junction zones" of the gel network) is possible. The zones, crystallized microdomains, are responsible for the highly non-Newtonian behavior of "strong" physical gels. The internal structure and morphology of the fibers have been obtained from (and their crystallographic polytypism[56] has been analyzed by) SAXS, SANS, and WAXS measurements of both gels and solids obtained by slow evaporation of their liquid component (xerogels).[49] "Head-to-head" contacts between the carboxylic acid groups allow the formation of multiple hydrogen-bonded sequences (Figure 3).

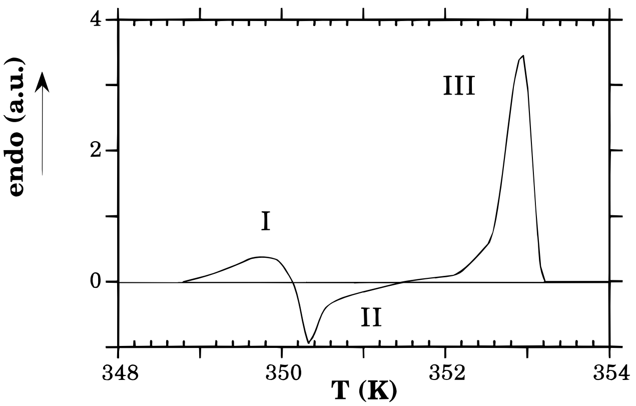

Figure 4. DSC trace of the mesomorphic solid made from gels of **1** in CCl_4 (heating rate: 0.31 K·min^{-1}). During heating, an endothermic process (I) transforms the mesomorphic xerogel to a more disordered solid. This is followed by crystal formation (exothermic process II) and, finally, crystal melting (sharp endothermic process III). Similar traces are observed with steroidal xerogels of **STNO** (see text). (Reprinted with permission from ref 47. Copyright 1980 Nippon Kagakki.)

The organization is monoclinic and sensitive to both the liquid type and the thermal/mechanical history of the samples. Xerogels are mesomorphic solids in which chiral, smectic-type helical structures exist in small domains;[47] DSC provides "thermal signatures" of local ordering (Figure 4).

1. Divalent or Trivalent Metal Salts of Fatty Acids

The thickening properties of various divalent or trivalent metal soaps, such as **C_{16}DP-Al** and **2**, have been utilized for many years in lubricating applications.[57] The degree of unsaturation and length of the lipophilic part of the gelator, the role of liquid-crystalline phase transitions (when they exist) on solubility in the liquid component as a function of temperature, the nature of the metal ion, and the type of liquid are some of the parameters that influence the solubility of metal ion soaps in organic liquids. Data from viscosity, fluorescence depolarization, osmotic pressure measurements[57] and stress-optical measurements,[58] show that the aluminum

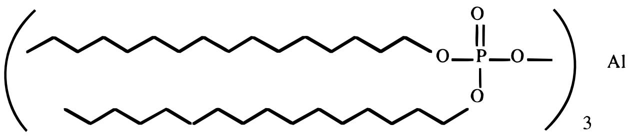

C_{16}DP-Al

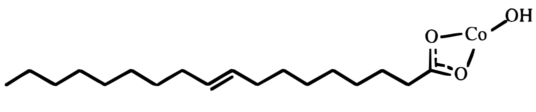

2

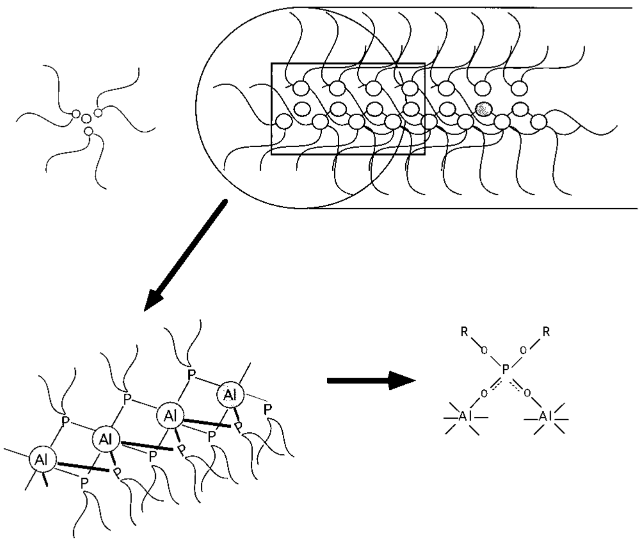

Figure 5. Model for **C_{16}DP-Al** cylindrical aggregates in *n*-hexadecane. (Reprinted with permission from ref 64. Copyright 1991 Academic Press.)

soaps form much larger micelles than soaps of mono- or divalent metals and suggest the existence of a specific interaction mechanism. Rheological data demonstrate that traces of water induce marked increases of viscosity through a possible sphere-to-long thread micellar transition in the dilute concentration range of the gelator. Further increases in water concentration to a 1/1 water/alkoxide molar ratio favor interlinking of the micellar soap through hydrogen bonding.

The gel structure was modeled as a network of threads interlinked by "junction points" and with continuous breaking and reforming processes.[57] Theories of the dynamics of reversible networks are available to correlate the microscopic lifetime of a junction and the macroscopic stress relaxation time[59,60] and can be tested with "weak gels". A well-characterized system of this type, a bicopper tetracarboxylate complex in cyclohexane,[61,62] will be discussed in a later section.

Aluminum disoaps form long chains in which the fatty carboxylate groups are almost perpendicular to a linear backbone of aluminum ions and hydroxyl groups.[63] Fibrous aggregates of gels of the aluminum salt of dihexadecyl phosphate (**C_{16}DP-Al**) in hydrocarbons have been observed by SEM. Even at 0.01 wt %, far below the critical gelator concentration, aggregates with stacking of trisubstituted aluminum atoms and three **C_{16}DP** groups are detectable; the aluminum ions are strongly coordinated by the phosphate bridges (Figure 5). Aggregation is lost upon addition of alkyl amines, which form links preferentially with the Al ions. Concentrated solutions of **C_{16}DP-Al** in *n*-hexadecane ($C > 18$ wt %) exhibit inverted hexagonal type H_{II} organizates.[64] The intercolumnar spacing between hexagonal arrays of the long cylinders varies from 27.5 Å (neat solid) to 54 Å (30 wt % **C_{16}DP-Al**), depending upon the hexadecane content.

Benzene and heptane solutions of 0.1−3 wt % **2** have been studied by viscometry.[63] Non-Newtonian shear thinning is followed by a Newtonian flow. The solutions, with no yield value, are viscoelastic and show a dramatic decrease of viscosity upon addition of pyridine or acetylacetone (i.e., molecules known to coordinate strongly with cobalt). This observation supports the hypothesis that coordination to cobalt leads to supramolecular aggregates. Furthermore, the decay curve of the transient electric birefringence of these systems reveals the existence of a broad spectrum of relaxation times of very polydisperse colloidal species. The rotational diffusion coefficient (D_r) of the rodlike chains is estimated to be 32 s^{-1} at infinite dilution. A mechanism of OH-bridging around a 4-fold coordinated cobalt, allowing connections between "monomeric" species in linear supermolecular aggregates, is proposed. Assuming tetrahedral symmetry for the CoO_4 unit, the mean aggregate length has been estimated and compared to the radius of gyration obtained from static light scattering measurements. Complementary electric birefringence studies of the rotational diffusion lead to an estimated mean persistence length for the semirigid chain ($l_p \approx 1080$ Å) and the weight-average number of Kuhn's segments ($L/l_p \approx 11$).

B. Steroid Derivatives

Some steroid derivatives[65] (such as deoxycholic, cholic, apocholic, and lithocholic acids and their salts) thicken aqueous salt solutions.[66] Similarly, some cholesteric esters and related derivatives, due to their molecular chirality, form thermotropic cholesteric (i.e., chiral nematic) mesophases.[67,68] These data infer that appropriately functionalized steroids should gel organic liquids. A remarkably simple example is dihydrolanosterol (**DHL**), which, at 1−10 wt %, gels various mineral, synthetic, animal, and silicone oils.[69] At 5 wt %, some simple esters of cholesterol, cholesteryl phenylacetate, and, to lesser extents, cholesteryl laureate and cinnamate also gel some silicone oils.[70]

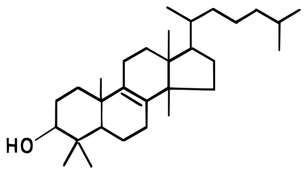

DHL

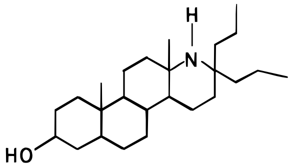

STNH

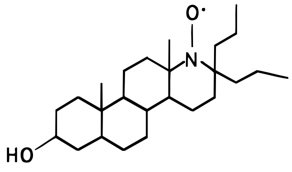

STNO

The first steroid-based gelator of hydrocarbons was discovered serendipitously during the course of the synthesis of a D-homosteroidal nitroxide free radical, D-3β-hydroxy-17,17-dipropyl-17a-azahomoandrostanyl-17a-oxy (**STNO**), from isoandrosterone derivatives.[71] Remarkably stable gels of hydrocarbon liquids can be made if the modified steroid has a

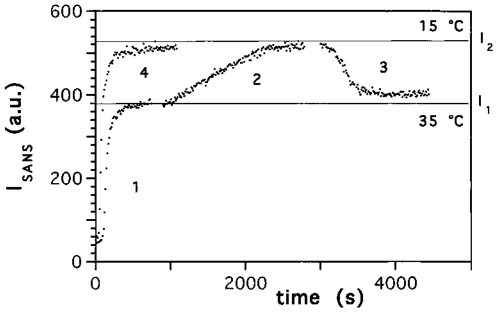

Figure 6. SANS curves for the kinetics of aggregation of the steroid **STNH** ($C_o = 5.9 \times 10^{-2}$ M) showing the additivity and reversibility of the gelation transition between 35 and 15 °C. (Reprinted with permission from ref 74. Copyright 1985 Academic Press.) (1) Sol-to-gel kinetic transition at 35 °C; (2) transition between 35 and 15 °C in the gel phase resulting from process 1; (3) transition from 15 to 35 °C in the gel phase resulting from process 2; (4) sol-to-gel transition at 15 °C. I_1 and I_2 are the equilibrium integrated scattered intensity within a low-angle window at 35 and 15 °C, respectively. The magnitude of I_{SANS} is correlated to the concentration of large fibrillar aggregates (see eq 2).

hydroxyl group at C_3 and an amine (**STNH**) or nitroxide functionality at the 17a-aza position. The gelling abilities of the steroids also vary with the position of unsaturated functionalities. Thus, two allyl groups at C_{17} inhibit gelation, but a double bond at $C_{5,6}$ does not. These steroids do not form gels in aromatic or polar liquids. Gel stability in saturated hydrocarbons (as indicated by the length of the period before solid–liquid phase separation, a thermodynamic course available to *all* of the gels described in this review) is very structure-dependent. Cyclohexane gels are stable for decades in sealed containers at room temperature.

EPR spectra of gels containing **STNO**[72] allow the fluid part (three narrow lines) and solidlike part (broad, shifted line) to be distinguished.[73] A partial phase diagram shows that the fraction of gelator not incorporated into the solidlike 3D network varies with temperature. It can be considered the "solubility limit" and includes the multiple dissolution/precipitation processes suffered by the aggregates. Details of the kinetics of aggregation have been examined in detail by using complementary techniques such as EPR, SANS (Figure 6), IR, and CD spectroscopies.[74] The methods take advantage of the spectral differences between isolated "monomeric" and aggregated states of the steroidal molecules. Aggregation and subsequent gelation do not occur immediately after a solution is cooled to a temperature in the gel domain of the phase diagram. The induction times and kinetics of the growth of the colloidal aggregates follow nucleation and growth laws used for unidirectional aggregates formed from supersaturated solutions.[74,75] A two-step homogeneous model can be used to simulate the kinetic curves, where the first step is autocatalytic and the second is first-order. Cooperativity is based upon the development of multiple hydrogen-bond sequences (at C_3). The kinetics of aggregation is dependent upon the supersaturation level (S) of the initial solution; growth of the microgel domains is in-phase for high S values and random for lower S values. As shown by neutron scattering experiments, the equilibration temperature of the gel (and not its thermal history) determines the amount of gelator involved in the solidlike network (Figure 6).

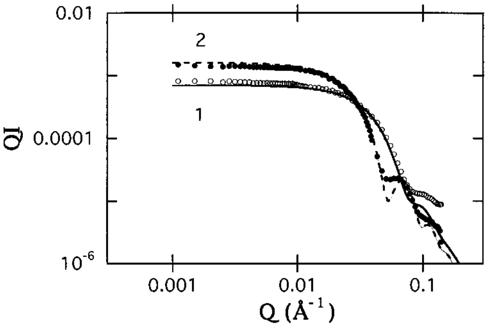

Figure 7. SANS of gels of **STNH**-based molecules in deuterated cyclohexane (1, o) ($C = 2.3 \times 10^{-2}$ g·cm^{-3} and in deuterated methylcyclohexane (2, •) ($C = 2.1 \times 10^{-2}$ g·cm^{-3}). Cross-sectional intensity QI *vs* Q is plotted. Points are experimental and lines are the best adjustments according to the full homogeneous cylindrical rod model described by eq 2. The influence of the liquid upon the structure of the aggregates is evident. (1) $r_o = 54$ Å, $\epsilon = 0.2$; (2) $r_o = 75$ Å, $\epsilon = 0.12$. (Reprinted with permission from ref 85. Copyright 1989 Editions de Physique.)

According to S, the time delay for complete aggregation can be from a few minutes to several hours. Arrhenius-type plots of the kinetic constants (from SANS, EPR, and IR data) provide activation energy values (*ca.* 6.5 kcal·mol^{-1}) consistent with a hydrogen-bonding mechanism.

SANS data show that the steroid aggregates are very long, rigid fibers, possibly symmetrical double helices of diameter 99 Å.[76] The cross sections of the fibers are approximately circular and rather monodisperse, as indicated by the existence of typical cross-sectional intensity oscillations in scattering curves at large angles (i.e., the Porod Q-range; Figure 7).

The "contact points" or nodes in the network are "junction zones" made by a specific overlap through fusion or coiling of two or more individual fibers over distances much longer than their diameters. This description is supported by freeze-fracture-etching transmission electron micrographs which show 91-Å diameter filaments (Figure 8A).[77–79] A helical substructure, consisting of two or more fibrils with a diameter of 46 Å, is also observed. Stereo TEM image pairs show spectacular views of the 3D porous structure of dilute gels. The images are very similar to those of gels with 1 wt % of an optically active glycolipid in water that are known to have strong intermolecular hydrogen bonds.[80] Analogous observations of helical fibers, random networks, protracted formation times following similar models, hydrogen-bonding interactions, and filament assembly processes have also been made for some naturally occurring systems like actin, tubulin, collagen, and DNA.[79]

TEM observations also provide insights concerning the structural relationship between aggregates in a native gel (with liquid) and in a dried xerogel.[52] Micrographs of entangled helical filaments with a *ca.* 580-Å pitch (Figure 8B) are found with very twisted fragments. Shrinkage of the gel network upon solvent evaporation is regulated by the elasticity and

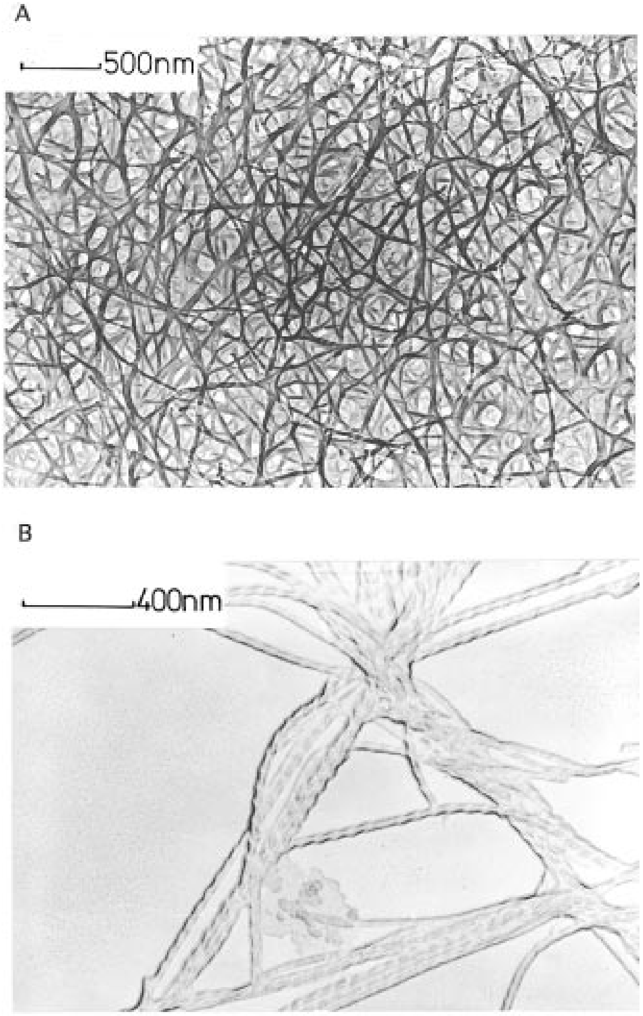

Figure 8. Electron micrographs of gels of **STNH** in cyclohexane. (**A**) Porous 3D gel network in cyclohexane. The main filaments of the gel network are *ca*. 91 Å in diameter (from refs 77 and 78 and Terech, P.; Wade, R. G., unpublished data). (**B**) Dried gel replica showing long twisted filaments and details of their interactions (from ref 52 and Terech, P.; Wade, R. G., unpublished data).

chirality of the fibers. Rearrangement of the chain trajectory of stress-sensitive chiral filaments involves helical folding of the fibers that collapse into super-aggregates, disruption of fibers and "junction zones", and an increase of the diameters of the chain fragments to three times the sizes found in native gels.

In the absence of external forces, strand networks of dilute gels are random. Anisotropically aligned networks in gels can be obtained either by allowing gelation to occur within strong magnetic fields of several Tesla or by employing concentrated solutions confined in thin sample holders.[81,82] Gels formed in the strong magnetic fields are unstable and separate readily into liquid and highly birefringent, collapsed, oriented filaments (Figure 9A). Changes in the rotational time constant for the rods and the time required for gelation (from rheological measurements) show that only the first stages of the sol-to-gel transformation are influenced by magnetic fields; rod orientation develops at the earliest stages of gelation. The order is "frozen" when the growing fibers overlap at C^*, but the initially formed (oriented) rods act as growth precursors for the remainder. Despite a small anisotropy of the diamagnetic susceptibility tensor of individual steroid molecules, the additivity property in a linear aggregate makes the ordering effect possible. The degree of alignment can be evaluated by optical microscopy under crossed polarizers or by wide-angle X-ray scattering (WAXS).

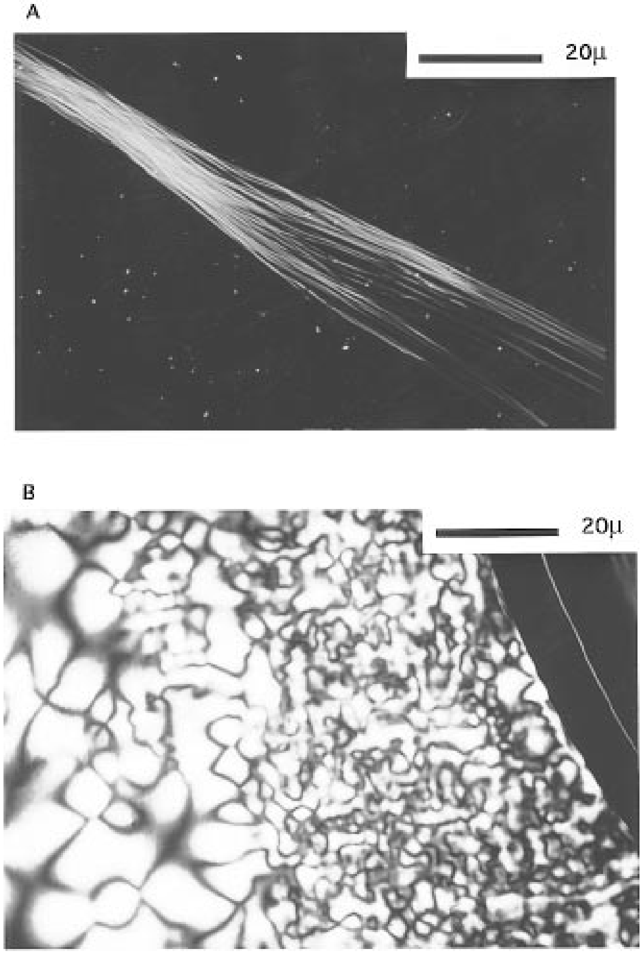

Figure 9. Optical micrographs (crossed polars) of gels of **STNH** in cyclohexane. (A) Oriented fibers separating from a gel formed within a 7 T magnetic field. (B) Schlieren textures observed in a 1-mm-thick gel ($C \approx 4$ wt %). The black portion is the air−gel interface. (Part A: Reprinted from ref 81. Copyright 1988 American Chemical Society. Part B: Reprinted with permission from ref 85. Copyright 1989 Editions de Physique.)

Substantial differences in the molecular organization of solid, gel, and xerogel states are apparent in gelation "signatures" from DSC, IR, optical polarizing microscopy, and WAXS techniques.[83,84] The xerogel is a mesomorphic organization which can be attained only through a solution-to-gel phase transition. Schlieren textures (Figure 9B), typical of nematic-like ordering, are observed for diamagnetic **STNH** while only extinction crosses confined within droplets are found for paramagnetic **STNO**. As in many other gel systems, small changes in the polarity balance of the gelator/liquid couple can induce nanoscopic structural and significant macroscopic changes. Additionally, steric properties of the liquid component can influence the aggregation process:[85] if cyclohexane is exchanged for methylcyclohexane or *cis*-decalin as the liquid, a ca. 50% increase of the filament diameter is measured by SAXS.

For gels of **STNH**, transmission electron micrographs and WAXS Bragg peaks, whose positions

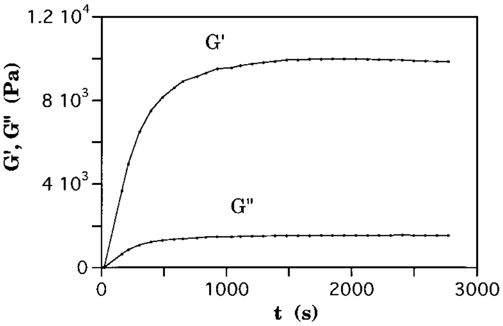

Figure 10. Rheological time sweep experiment for a **DDOA**/octanol gel. The warmed solution ($C = 0.98$ wt %) was introduced between the cone and plate of the rheometer and cooled to 20 °C. Frequency = 1 Hz, angular displacement $\alpha = 6.9 \times 10^{-4}$ rd, strain amplitude $\gamma = 1\%$. (Reprinted with permission from ref 90. Copyright 1995 Academic Press.)

depend on the sample's history (e.g., age, liquid, and concentration) indicate that fiber interactions are (pseudo)crystalline (lyotropic) zones in a heterogeneous network, with a solidlike behavior. Attempts to determine the symmetry relationships among the orthorhombic crystallographic organization of the neat solid, the gel, and xerogel states of **STNH** are in progress.[86]

C. Anthryl Derivatives

2,3-Bis-*n*-decyloxyanthracene (**DDOA**) is able to gel various alkanes, alcohols, aliphatic amines, and nitriles.[87] The related anthraquinone **3** is also a gelator but the 2,3-dialkoxynaphthalene is not. The solution-to-gel phase transition of **DDOA** varies over a wide range of temperatures, depending on the liquid and gelator concentration. **DDOA** is also of interest due to its photochromic properties.[88,89] The onset of formation of a 3D, elastically-connected network of **DDOA** aggregates has been followed by rheological measurements.[90] There is an abrupt increase of the storage modulus (G') at a characteristic time of the aggregation process (Figure 10).

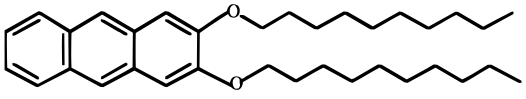

DDOA

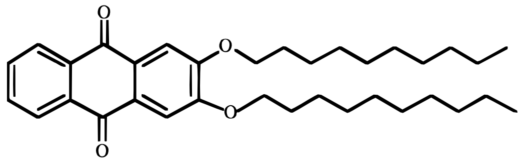

3

The magnitude of the equilibrium value in 1-octanol, G'_{equ} (*ca.* 10^4 Pa for $\phi \approx 0.01$), is much larger than the loss modulus, G''_{equ} (*ca.* 1500 Pa). Comparison of the magnitude of the elasticity of the gel network with that of other systems suggests that the interaction zones are permanent crystalline microdomains at a given temperature. When cycled between 20 and 40 °C, the mechanical properties of the **DDOA**/1-octanol system exhibited hysteresis. Below T_{SG}, its elasticity at low frequency and large yield-stress value ($\sigma^* \approx 550$ Pa for $\phi = 0.01$) are consistent with the self-supporting ability expected of a solidlike gel.

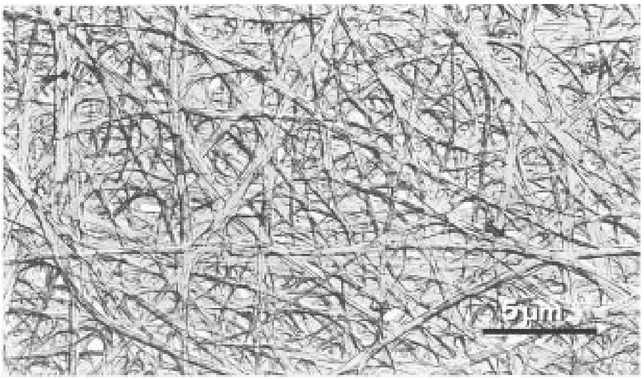

Figure 11. Freeze-fracture electron micrograph of gels from **DDOA** and propanol. (Reprinted with permission from ref 89. Copyright 1992 Allen Press.)

DDOA gels ($\phi \approx 0.02$) in butanol-d_{10} and decane-d_{22} exhibit comparable isotropic SANS patterns with a monotonous decrease ($I = Q^{-3.7}$) from low to higher angles, where diffraction peaks (for instance, at $Q \approx 0.1$ Å^{-1}) are observed. Since neutron nuclear contrasts of **DDOA** aggregates in the two liquids are comparable, the experiments describe the part of the morphology that is insensitive to the liquid type. A Porod analysis shows a broad bump ($0 < Q < 0.075$ Å^{-1}) attributed to the form-factor of the **DDOA** aggregates and whose width is related to the size polydispersity of the scatterers. The peaks at larger angles ($Q \approx 0.1$ Å^{-1}) are due to the structure factor of ordered heterogeneities in the gel network. The bump can be modeled as an interfacial scattering from a distribution of diameters ranging from ~100 to 500 Å.

Freeze-fracture electron micrographs of **DDOA**/propanol gels indicates the presence of a dense, 3D, random network of fibrous rigid bundles with 600–700-Å diameters (Figure 11). At least in part, the thick fibers may be a consequence of syneresis. When submitted to mechanical stress, **DDOA**/acetonitrile gels shrink significantly.[86]

The network structure and related swelling or shrinking of the gel is a result of a balance of forces, including its elasticity, aggregate–aggregate affinity, and possibly additional ones influencing the osmotic pressure of the gel (such as the degree of ionization in very polar liquids).

A better understanding of the "junction zones" has been derived from WAXS studies of powdered **DDOA**. The diffraction pattern exhibits a sequence of Bragg peaks at 0.095, 0.166, 0.191, 0.254, 0.287, and 0.336 Å^{-1} whose spacings are in the ratios $1:\sqrt{3}:\sqrt{4}:\sqrt{7}:\sqrt{9}:\sqrt{12}$ (typical of hexagonal ordering).[91] **DDOA** in gel strands is also crystalline since Bragg peaks from the gel and neat solid are located at the same positions. The *[11]* reflection (associated with a reticular distance $\langle d \rangle \approx 66.1$ Å), corresponding to an intercolumnar distance of 76.3 Å in a hexagonal array, may arise from crystalline junction zones formed by bundles of aggregates; they are "dry" crystalline microdomains, free of swelling by the liquid.

D. Gelators Containing Steroidal and Condensed Aromatic Rings

In contrast to the steroids **STNH**, **STNO**, whose gelation ability relies upon the presence of a hydroxyl group at C_3, another class of molecules (**ALS**) which are functionalized at C_3 and cannot be H-bond donors are also efficient gelators of many types of organic liquids. They consist of an aromatic group (**A**) connected to a steroidal moiety (**S**) via a linking group (**L**). In most cases, the **A** group at C_3 contains fused aromatic rings. In principle, the **ALS** permit an analysis of the contribution of and competition between the **A** and **S** autoassociative parts on a mechanistic level since they are able to impart to gels on a mesoscopic level some of their molecular attributes (e.g., an ability to luminesce and to sense chiral interactions).

1. Anthryl and Anthraquinone Appended Steroid-Based Gelators

Cholesteryl 4-(2-anthryloxy)butanoate (**CAB**) and cholesteryl anthraquinone-2-carboxylate (**CAQ**) are examples of **ALS** molecules whose linking groups enable them to adopt an overall rodlike shape. **CAB** forms gels with organic liquids that are hydrocarbons, alcohols, aldehydes, esters, amines, etc. (Table 1).[92] Both **CAB** and **CAQ** gel more complex fluids, like silicone oils, also.[93,94] Many **CAB** gels are luminescent and some are metastable, exhibiting a gel-to-liquid/solid phase separation after variable periods of time.

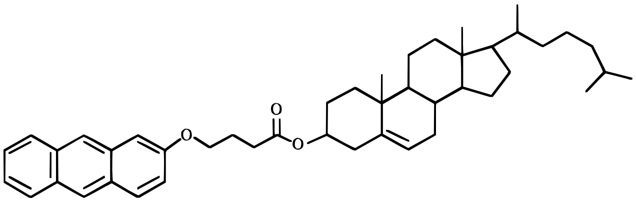

CAB

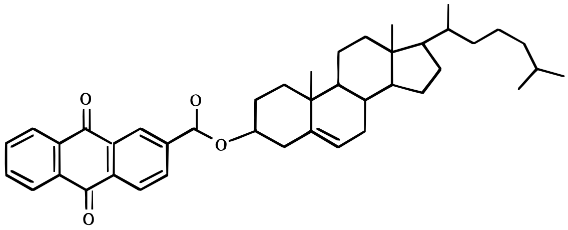

CAQ

Gelation abilities have been correlated with the three structural components of a wide variety of **ALS** molecules.[95−97] For instance, neither a 1-pyrenyl analogue of **CAB** (containing four nonlinearly fused rings in the **A** portion) nor a 2-naphthyl anologue of **CAQ** (containing only two fused rings) was capable of gelling any of a variety of liquids; the shape and nature of the ring systems in the **A** part are important considerations in gelator design. Gelation temperatures (T_{SG}) have been measured from changes in luminescence, absorption, and dichroic intensities.

Table 1. Organic Liquids Tested for Gelation by CAB

liquid	wt % of **CAB**	phase formation[a]
1-bromopropane	1.4	N
1-bromo-3-phenylpropane	1.54	N
pentane	1.20	Y (5 °C)
hexane	0.80	Y
heptane	0.80−2.7	Y
octane	0.81	Y
dodecane	0.10	N (sol)
	0.25−4.1	Y
tetradecane	2.23	Y
hexadecane	0.81−2.9	Y
heptadecane	3.00	Y
octadecane	2.70	Y
eicosane	1.57	Y
isooctane	0.81	Y
cyclohexane	1.41	Y
methylcyclohexane	0.80	Y
decalin	1.56	Y
1-tetradecene	1.50−4.8	Y
1-propanol	1.50	Y
1-dodecanol	1.52	Y
1-octanol	0.80	Y
1,3-propanediol	1.09, 1.33	N
benzyl alcohol	1.50	Y
4-heptanol	1.53	Y
2-butene-1,4-diol	1.33	N (ppt)
3,3-dimethyl-2-butanol	1.43	N (sol)
	0.72	Y (5 °C)
heptanal	1.51	Y
nonanoic acid	1.61	Y
valeric acid	1.47	N (sol + ppt)
n-pentyl acetate	1.51	N (soln)
		Y (5 °C)
n-butylamine	1.50	N (sol)
		Y (5 °C)
benzylamine	1.46	N
		Y (5 °C)
N-methylbenzylamine	1.25	N (soln)
		Y (5 °C)
α-methylbenzylamine	1.49	N (soln)
		Y (5 °C)
benzene	1.50	N (soln)
toluene	1.33−2.31	N (soln)
7-tridecanone	1.48	N (ppt)
2-octanone	0.99−1.55	N (ppt)
2-undecanone	1.54	N (ppt)
4-heptanone	1.53	N (ppt)
1,2-dimethoxyethane	1.46	N (ppt)
		Y (<−10 °C)
1,3-pentadiene	1.46	N (soln)
		Y (<−10 °C)

[a] Y = gel formed at room temperature unless noted otherwise; N = no evidence of gel formation; sol = sol formation; ppt = precipitate; soln = isotropic-like solution.

In **CAB**/*n*-alkane gels, T_{SG} is independent of liquid chain length. However, the lifetime of a gel at room temperature in a sealed vessel (to avoid evaporation) is dependent upon gelator concentration and liquid type. For instance, the stability in cyclohexane is lower than in *n*-alkanes. By contrast, the stability of **STNH**/cyclohexane gels is *much* greater than of **STNH**/*n*-alkane gels.[85]

Absorption and fluorescence from the anthryloxy group provide information on the local ordering of **CAB** molecules in aggregates of the gel phase. New absorption bands, from excitation dipole coupling between anthracenyl groups stacked face-to-face within the aggregates, can be observed. Neighboring **CAB** molecules overlap partially, with their long molecular axes nonparallel. When the liquid "quality" or polarity is varied (N.B. hexadecane and

1-octanol), significant spectral differences in the fluorescent properties of the gels can be detected.[98]

Furthermore, the sol and gel phases of **CAB** in 1-octanol/hexadecane mixtures have been studied by using the position, shape, and intensity of absorption and emission features.[98] At 75/25 or lower 1-octanol/hexadecane ratios, T_{SG} is the same as in neat hexadecane; at 80/20 or higher ratios, T_{SG} can be that found in neat hexadecane or in neat 1-octanol depending upon the thermal history (slow or fast cooling rate) of the sample. Based upon these and other observations, it was concluded that two types of morphologies can exist; a configurational transition which is liquid-dependent occurs in an abrupt, stepwise fashion.

Transient, birefringent textures (faint focal conic patterns, evolving to fan-like textures or Maltese crosses) have been observed by polarized optical microscopy for **CAB** and other **ALS** samples cooled from above T_{SG}. They indicate that the steps leading to the dispersed gel state may include formation of a lyotropic cholesteric phase.[99] Neat **CAB** and some (but not all) other successful **ALS** gelators form thermotropic cholesteric liquid-crystalline phases.[100]

CD measurements on **CAB** gels with hexadecane and 1-octanol suggest the presence of helical structures. At the same time, ^{1}H NMR experiments provide no evidence for impaired liquid mobility on the molecular scale. Interactions of the proton-donor liquid, 1-octanol, and specific parts of **CAB** are suspected to contribute to strand twists that are absent when n-alkanes are the liquid.

In addition to being thermally reversible, some organogels with low molecular mass gelators are also *thixotropic*;[101] when sufficient stress is applied isothermally, they form a sol that reverts at rest to the gelled state. As an example, thixotropic gellike suspensions are obtained with a low molecular mass zinc(II) trisubstituted porphyrin in cyclohexane (vide infra).[102]

There is also one example of the *induction* of *thixotropy* (i.e., the ability of a viscoelastic jelly at rest to be converted reversibly to a viscous liquid by a simple mechanical stress like shaking). Gels of **CAQ** are not thixotropic. However, when a small amount (<1 wt %) of cholesteryl 9,10-dimethoxyanthracence-2-carboxylate (**CMAQ**), a nongelator, is added to normal recipes of **CAQ** and 1-octanol or hexadecane, thixotropic gels are obtained.[103] As neat solid mixtures, **CAQ** and **CMAQ** form charge-transfer complexes whose characteristic absorption can be detected visually. Thixotropy in the "crystalline gels" ("strong gels") is thought to arise via preferential formation of the complexes at and near junction zones. When these mixed crystalline segments are disturbed mechanically, they cleave, yielding a sol, but reattach themselves with time. Long-range interactions between short rods in viscoelastic liquids ("weak gels") are thought to account for thixotropy in the zinc(II) trisubstituted porphyrin in cyclohexane.

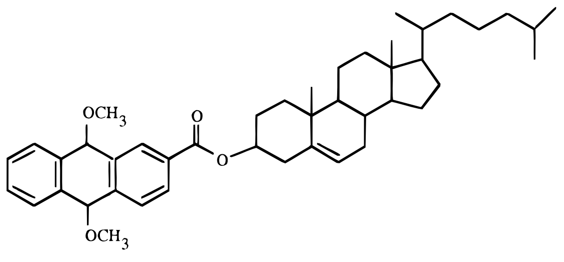

CMAQ

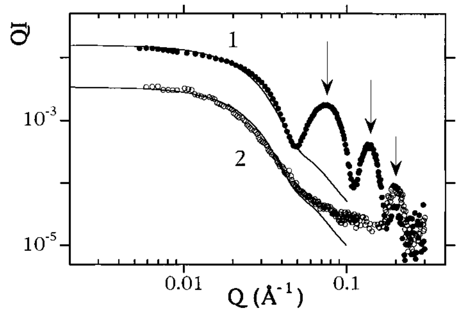

Figure 12. SAXS cross-sectional intensity *QI versus Q* plots for **CAB** organogels. (1, ●) decane, $C = 0.0192$ g·cm^{-3}; (2, ○) octanol, $C = 0.010\ 58$ g·cm^{-3}. Intensity for decane is multiplied by 13 for the sake of clarity. Lines are best fits according to expression (2): (1) $r_o = 82$ Å, $\epsilon = 0.24$; (2) $r_o = 85$ Å, $\epsilon = 0.24$. ϵ is the radial Gaussian dispersity of the cross sections. The diffraction peaks of the lyotropic microdomains in the decane network are marked by arrows. (Reprinted with permission from ref 104. Copyright 1995 American Chemical Society.)

SANS and SAXS scattering techniques are most consistent with nanoscopic TEM, CD, and other spectroscopic measurements.[104,105] The SANS scattering profiles (Figure 12), coupled with the similarity of the neutron contrast values of **CAB** aggregates in deuteriated decane and 1-butanol, support the previous conclusions that the liquid type can cause significant structural changes in the gels. *QI vs Q* scattering curves of **CAB**/1-butanol and **CAB**/decane gels exhibit a low-angle plateau typical of the form-factor of long and rigid fibers (eq 2). A Guinier analysis provides values for the cross-sectional radius of gyration (R_c). Assuming homogeneous circular cross sections, the strand diameters are calculated to be 192 Å in alcohols and 160 Å in alkanes. Since SANS and SAXS data provide slightly different R_c values (59 *vs* 54 Å, respectively) for **CAB**/decane gels, the cross-sectional contrast profiles may be heterogeneous. The larger Q-value part of the scattering curve, with broad peaks, comes from the structure factor of ordered heterogeneities in the network. Consequently, the full scattering curve results from mixing of the form-factor of the **CAB** fibers (low-angle part) and the structure factor (wide-angle part) of ordered domains. The low-angle fit, according to eq 2, and the Guinier and Porod analysis give a consistent picture of the **CAB** aggregates in alcohols. Calibrated neutron intensities provide an estimation of the number of **CAB** molecules per unit length ($n_L = M_L/M$) of fiber in alcohols.[104] The value of n_L, ca. 18 molecules·Å^{-1}, is close to that for packing in the solid state, ca. 19.1 mol·Å^{-1}, assuming a cylinder of **CAB** molecules. The two estimates are very close in spite of the fact that scanning electron micrographs and SAS data show that the fibers are not cylindrical.

Crystalline **CAB** powder exhibits Bragg reflections (at 0.096, 0.163, 0.188, 0.248, and 0.281 Å^{-1}) are in

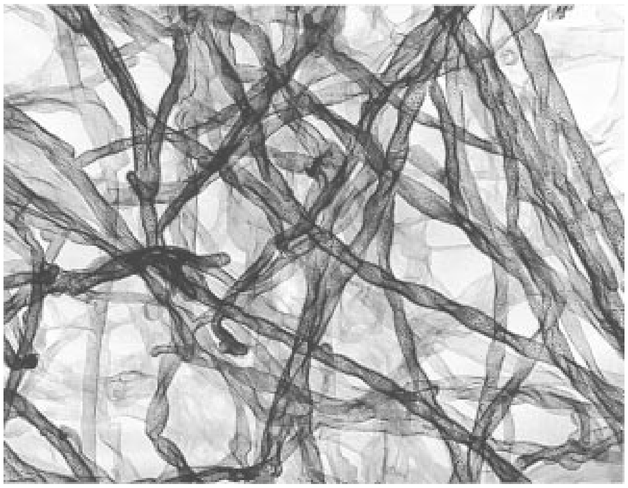

Figure 13. Electron micrograph of **CAB** in 2-octanol (Fee, C.; Lin, Y.-c.; Kashar, B.; Weiss, R. G., unpublished data). The cross-sectional dimensions of the twisted fibers are virtually the same as those for 1-octanol (263 × 82 Å). (Reprinted from ref 96. Copyright 1989 American Chemical Society.)

the ratio $1{:}\sqrt{3}{:}\sqrt{4}{:}\sqrt{7}{:}\sqrt{9}$, indicating hexagonal ordering. The intercolumnar distance in the neat solid is $D_0 = (2/\sqrt{3})\ 21/Q_{(11)} = 75.7$ Å, where $Q_{(11)}$ is the first reflection generated by a two-dimensional hexagonal array of scatterers. The gel **CAB** network appears to be heterogeneous and comprised of fibers "interconnected" by swollen lyotropic microdomains (intercolumnar distance 102.2 Å; diameters of the connecting fibers ca. 160−170 Å). Spacings of peak positions characterizing the swollen lyotropic organization are in the ratio 1/1.92/2.75. From SAXS diffraction patterns of **CAB**/1-butanol gels, molecular packing in the aggregates is different from that in both the neat solid and the **CAB**/decane aggregates.

The nodes of **CAQ** organogel networks are lyotropic microdomains that vary from hexagonal (decane) to more compact, lamellar-like ordering (1-octanol).[105] Schlieren optical textures confirm the inhomogeneity of the orientation of the thread-like structures, and CD spectra resemble those of neat **CAQ** solid, cooled from its mesophase. However, the solid morph obtained from solvent crystallization is packed differently from the gel strands.[35]

Comparison of the molecular length of **CAB** (*ca.* 38 Å) and the characteristic lengths calculated from SAS data (*vide ante*) indicate that molecular pairs are involved in the columns of the solid state while, in gels, more molecules are associated. Micrographs of freeze-fractured and etched samples (Figure 13) show a 3D network of fibrous bundles emanating from central points. The dimensions of the rectangular cross-sections of the fibers, 209 × 104 Å in dodecane (non-twisted) and 263 × 82 Å (twisted) in 1-octanol,[96] correspond approximately to the cross-sectional areas determined by SANS. Additional specific effects, such as inhibition of gel formation, preaggregation in sols, and crystallization have been observed when sample holders are narrowed to widths comparable to or smaller than the diameters of the colloidal units of strands.[98]

Liquid molecules are included in some strands, and their swelling (by hydrocarbons) may be due to molecular shape and electrostatic compatibility with the lipophilic external shell of **ALS** and other steroid-based organogelators.[106] When swelling is not possible (for instance when a gelator, such as **DDOA**, lacks a steroidal part), gels with "dry crystalline nodes" (involving stacks of oriented **DDOA** anthryl groups) are formed, and diffraction patterns of the solid and gel phases are almost superimposable. For networks with nodes involving lyotropic microdomains, the diffraction peaks are broadened and shifted to an extent that depends on the liquid type and its concentration within the strands.[104,105]

A "molecular engineering" approach to gelation has been attempted to identify the influence of the different segments of **ALS** molecules on the gelation process.[95,107] Parameters such as the α/β stereochemistry at C_3, the nature of the alkyl chains on C-17 of the **S** part, and the length and functionality of the **L** part have been examined; see, for example, **4**−**9**. Gelation ability seems favored by β stereo-

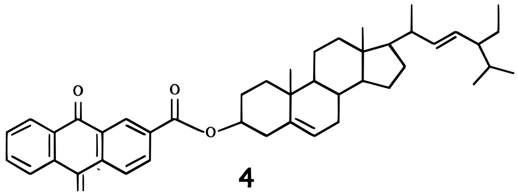

4

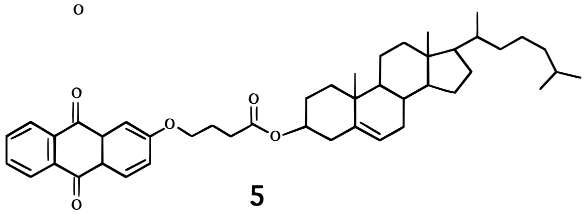

5

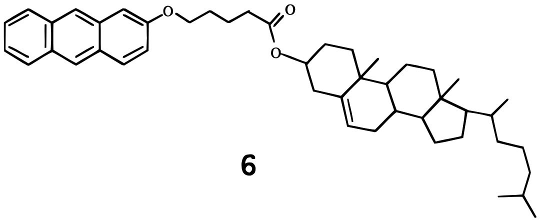

6

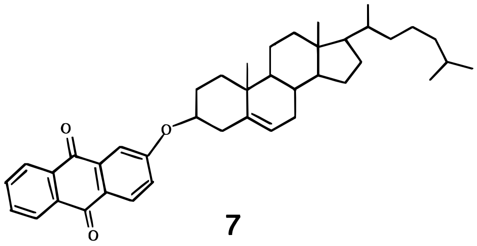

7

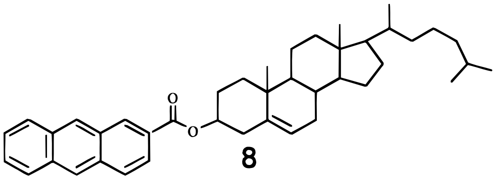

8

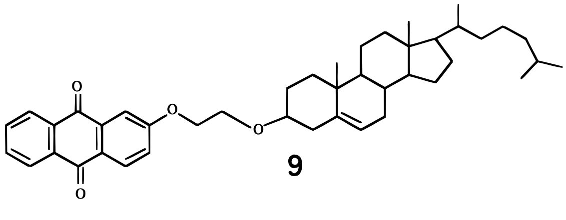

9

chemistry at C_3 while changes at C_{17}, as long as they are minor (e.g., introduction of unsaturation or an ethyl substituent), do not have a large impact.

The contribution of the steroidal moiety to gelation can be analyzed by comparing **CAB** and **DDOA** in their solid states. Since the powder X-ray diffraction patterns are almost superimposable, the factors associated with interactions of the aromatic parts (and their somewhat flexible **L** groups) play a crucial role in determining the structure of the ordered condensed states.

2. Azobenzene Steroid-Based Gelators

Molecules having a highly polar azobenzene group linked at C_3 of a steroidal moiety (e.g., **10**−**13**) have been found to gel liquids such as ethanol, acetic acid, amines, dichloromethane, ethers, and esters (Table 2).[108] The α- and β-anomers preferentially gel apolar and polar liquids, respectively. As frequently observed with fiber-like aggregates of optically active molecules,[96,109] CD (free of linear dichroic effects) can be used to follow aggregation at the *microscopic* scale at the same time that *macroscopic* gelation is occurring and to explore enantiomorphic relationships. For instance, from the positive exciton coupling band observed for the α-anomer (**10**), it can be deduced

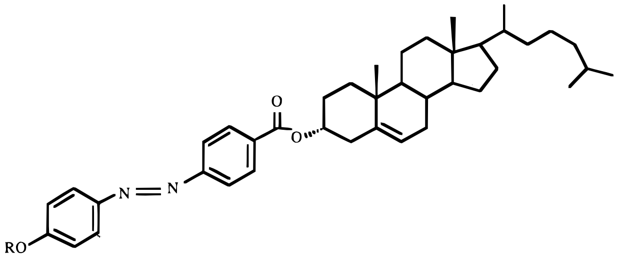

10

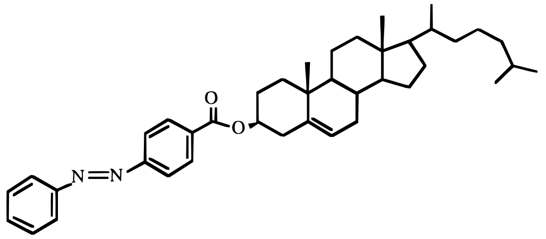

11

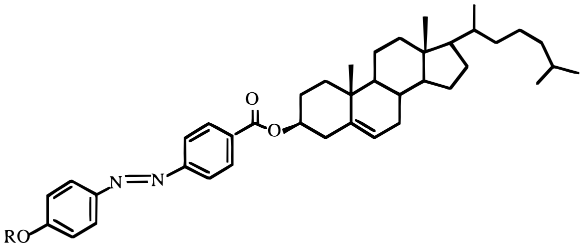

12

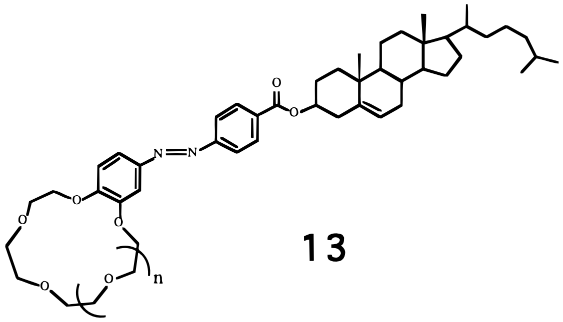

13

Table 2. Organic Liquids Tested for Gelation by 10 Homologues[a]

liquid	R MeO	EtO	PrO	BuO	PeO	DecO
n-hexane	Gf	G	G	G	G	G
n-heptane	Gf	G	G	G	G	G
n-octane	Gf	G	G	G	G	G
paraffin	G	G	G	G	G	G
cyclohexane	S	S	S	S	S	G
methylcyclohexane	S	Gf	Gf	Gf	G	G
decalin	S	S	S	Gf′	Gf′	G
carbon tetrachloride	S	S	S	S	S	S
carbon disulfide	S	S	S	S	S	Gf′
benzene	S	S	S	S	S	S
toluene	S	S	S	S	S	Gf′
p-xylene	S	S	S	S	S	S
nitrobenzene	S	S	S	S	S	G
m-cresol	S	S	S	S	S	Gs
1,2-dichloroethane	S	S	S	S	S	Gs
dichloromethane	S	S	S	S	S	S
chloroform	S	S	S	S	S	S
diethyl ether	S	Gs	S	Gs	G	G
dipropyl ether	S	Gf′	Gf′	Gf′	Gf′	G
diphenyl ether	S	S	S	S	S	G
tetrahydrofuran	S	S	S	S	S	S
1,4-dioxane	S	S	S	S	S	G
ethyl formate	Gf	G	G	G	G	G
methyl acetate	S	G	G	G	G	G
ethyl acetate	S	Gf	Gf	Gf	G	G
ethyl malonate	S	G	G	G	G	G
acetone	G	SG	G	G	G	SG
methyl ethyl ketone	S	G	G	G	G	G
N,*N*-dimethylformamide	G	SG	G	G	G	SG
N,*N*-dimethylacetamide	G	G	G	G	G	G
dimethyl sulfoxide	SG	G	G	G	G	SG
N-methyl-2-pyrrolidone	S	Gf	Gf	Gf	G	G
acetonitrile	SG	SGc	SGc	SG	SG	SG
methanol	SG	SGc	SGc	SG	SG	SG
ethanol	SG	SGc	SG	SG	SG	SG
1-propanol	G	SG	SG	SG	SG	SG
1-butanol	G	SG	SG	SG	SG	SG
1-octanol	G	G	G	G	G	SG
benzyl alcohol	G	G	G	G	G	G
acetic acid	G	SGc	SGc	SG	SG	SG
hexanoic acid	S	S	S	S	S	G
acetic anhydride	G	SG	SG	SG	G	SG
propylamine	S	Gf	S	S	S	G
diethylamine	S	S	S	Gf′	Gf	G
triethylamine	S	Gf′	Gf′	Gf′	Gf′	G
aniline	S	Gs	Gf′	S	Gf	G
pyridine	S	S	S	S	Gs	G
triethylsilane	G	G	G	G	G	G
trimethylchlorosilane	S	Gf′	Gf′	Gf′	Gf′	G
dimethylpolysiloxane(1cs)	G	SG	SG	SG	SG	SG
dimethylpolysiloxane (6cs)	G	SG	SG	SG	SG	SG
cyclomethicone	G	SG	SG	SG	SG	SG
trifluoroethanol	G	SG	SG	SGs	G	R
glycerol	I	I	I	I	I	I
water	I	I	I	I	I	I

[a] [Gelator] = 1−7 wt %; G = gel formed when cooled at 2−20 °C and stable at room temperature; Gc = gel formed but became crystals at room temperature; SG = gel was formed at [gelator] < 1 wt %; Gf = gel formed when cooled in a refrigerator (at −6 °C) and stable at room temperature; Gf′ = gel formed when cooled in a refrigerator (at −6 °C) but not stable at room temperature; gel not formed because of crystallization (R), gelator dissolved at room temperature (S), or gelator insoluble upon heating (I).

that the dipoles of the azobenzene parts in the aggregate are associated in a clockwise fashion (*R*-chirality). The cooling rate of samples initially above T_{SG} can affect the sign of the gel CD spectra; metastable structures are formed as in the case of **CAQ** gels in hexadecane/1-octanol mixtures.[98] Attempts to correlate strand helicity with the cooling rate and the α/β-anomeric nature of the link to cholesterol have been made on the basis of SEM observations. The absolute configuration at C_3 has also been shown to be an important factor in the aggregation modes of monolayers developed at the air–water interface.[110] As witnessed by the greater efficiency of gelators with an odd number of carbon atoms on a group attached to the azobenzene moiety, there is a delicate lipophobic/lipophilic structural balance governing gelation.

An aggregation model for fiber-like helical aggregates, in which the association of the chiral cholesterol moieties constitutes the primary driving force, is proposed. The β-anomer of the gelator favors additional interactions, strengthening the aggregate through face-to-face orientations of the azobenzene moieties. Consequently, the stability of the gels and the aggregative and gelling properties of the β-anomers are greater than those of the α-anomers while the solubility of the β-anomers is lower. The test-tube tilting method, the ball-drop method, and the spectroscopic turbidity method have been used to determine the gel-to-sol phase transition temperatures (T_{GS}) over a part of the phase diagram.[108] The related gel-to-sol phase transition can be envisioned as a dissolution process of crystals in which the melting energy can be deduced from measurements of T_{GS} as a function of concentration (eq 1). Reversible sol-to-gel phase transitions, induced by *trans*–*cis* photoisomerization of the azobenzene groups, can be monitored by CD spectroscopy.

The insensitivity of T_{SG} of gels containing one of **10**–**13** to the nature of the liquid component indicates that solvent molecules do not participate in the structures of the gelator strands (i.e., they have molecular packing like in the neat solid, as found for some fatty acids[49] and anthracenyl-containing molecules[106]). However, this conclusion cannot be generalized[35] and is most suspect when lyotropic organizations participate in a gel network.

As mentioned, structural variations of the functional group linked to cholesterol allow investigation of the gelation mechanism. In this regard, specific derivatives can be used for chiral recognition since they are capable of forming gels of differing stabilities (as estimated by T_{GS}) when mixed with enantiomers of chiral monosaccharides.[111]

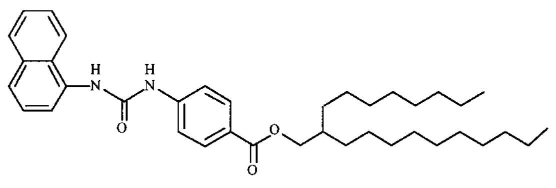

14

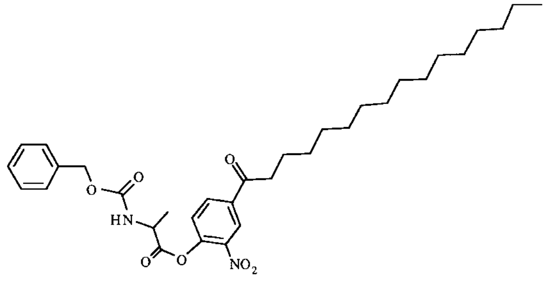

15

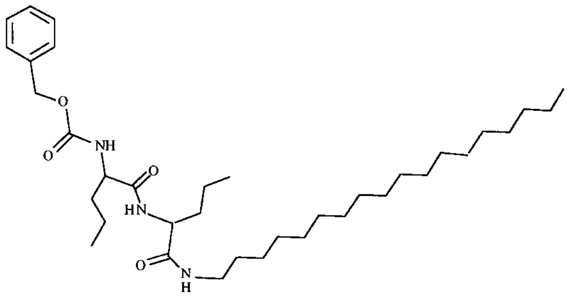

16

$H\text{-}(NH\text{-}CH(R)\text{-}C(O))_{n}\ NHC_{m}H_{2m+1}$

17

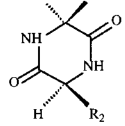

18

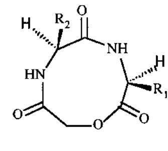

19

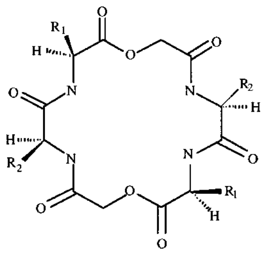

20

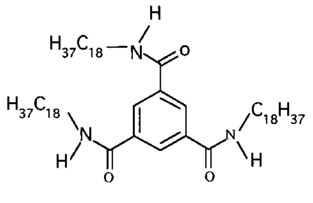

TSTA

E. Amino Acid-Type Organogelators

*2-Octyldodecyl 4-[[(1-Naphthylamino)carbonyl]amino]benzoate (**14**).* Ca. 4 wt % of **14** forms nematic-like lyotropic gels.[112] Their T_{GS}, probed by DSC, is slightly higher than that determined by birefringence (Δn) studies (which measure the temperature (T_{NI}) at which $\Delta n \rightarrow 0$). Schlieren textures, associated with a small birefringence ($\Delta n \approx 10^{-4}$), and shear induced birefringence can be observed when samples are temperature quenched. Slowly cooled samples remain isotropic but become uniformly birefringent when annealed. The correlation between the cooling rate of the gelling sample and the size of the nanoscopic structures suggest that metastable states[98] can be formed.

*N,N′,N″-Tristearyltrimesamide (**TSTA**) and Related Molecules.* Low concentrations of **TSTA** gel a variety of polar liquids, including 1,2-dichloroethane,

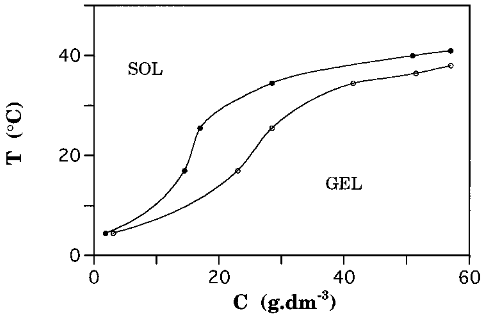

Figure 14. Sol-to-gel phase transition temperatures of *N*-benzyloxycarbonyl-L-alanine-4-hexadecanoyl-2-nitrophenyl ester (**15**) in (o) methanol or (●) cyclohexane versus gelator concentration (***C***). (Reprinted with permission from ref 114. Copyright 1992 Royal Society of Chemistry.)

nitrobenzene, dimethyl sulfoxide, and *N*,*N*-dimethylformamide via the formation of typical 3D strand networks.[113] Relatively sharp heating endotherms and cooling exotherms (at lower temperatures) can be detected by DSC. Analogous structures in which methyl and stearyl groups are placed on the amide nitrogen atoms or the stearyl groups are replaced with shorter chains result in molecules that are much less efficient gelators. Infrared spectra of **TSTA** gels and isotropic solutions demonstrate that aggregation involves extensive intermolecular hydrogen bonding.

*N-Benzyloxycarbonyl-*L*-alanine 4-Hexadecanoyl-2-nitrophenyl Ester (**15**).* Compound **15** gels methanol and cyclohexane through networks of intermolecular hydrogen bonds between N—H and C═O parts of the urethane group.[114] Dipole−dipole interactions between NO_2 and C═O (at the 4-position) groups as well as the presence of long hydrocarbon chains are important contributors to the aggregation process.

Long-Chain Alkylamide Derivatives. *N*-Benzyloxycarbonyl-L-valyl-L-valine *n*-octadecyl amide (**16**) gels many organic liquids.[115] IR spectra show extensive intermolecular hydrogen bonding (broad band at $\nu \approx 3290$ cm^{-1}), and the enthalpic contribution deduced from the phase diagram (Figure 14) is compatible with the participation of at least two of the three theoretically available hydrogen bonds per molecule (between N—H and C═O groups). Structural parameters that determine the efficiency of amino acid-based gelators (and the helicity of their aggregate strands[116]) are chirality, structure of the amino acid residue, and the configuration of the lipophilic tail. As noted in aqueous systems,[54,117,118] many (but not all[49]) racemic mixtures of efficient, optically active gelators can be used also.

Oligomeric α-Amino Acid Gelators. A wide variety of organic liquids can be thickened by oligomers of some amino acid derivatives. Their efficiency depends on the degree of oligomerization, the hydrophibicity of the C-end and N-end groups, and the functionality of the α-carbon atom.[119,120] Thermodynamic parameters have been deduced from the phase diagram of **17** (R = $CH_2CH_2CO_2Me$; $n = 4.2$; $m = 12$). Typical values in nitrobenzene, $\Delta H(25\ °C) \approx -23.2$ kJ·mol^{-1} and $\Delta S(25\ °C) \approx -21.2$ J·K^{-1}·mol^{-1}, indicate that two hydrogen bonds per acid residue are formed. For rather long oligomers of glutamates, CD spectra show that a β-conformation is adopted through intermolecular hydrogen bonding; α-helical and random coil conformations are inefficient for gelation.

Cyclo(dipeptide)s. Compounds of structure **18** (where R_1 and R_2 can be a variety of alkyl groups),[121] have four hydrogen-bonding sites per molecule. Similar compounds consisting of more than one amino acid or having branched alkyl groups are more efficient gelators of organic liquids than cyclodimers. As with other classes of gelators, branching and bulkiness of alkyl substituents appear to affect gel stability by moderating the aggregate−aggregate interactions which promote crystallization. IR spectra reveal the presence of H-bonds and TEM confirms the existence of fiber-like aggregates. Slow evaporation of a CCl_4 gel of **18** ($R_1 = CH(CH_3)_2$ and $R_2 = (CH_2)_2CO_2(CH_2)_2CHMe(CH_2)_3CHMe_2$) produces xerogels in the form of translucent films structured in layers separated by 19.3 Å in a ladder-like aggregate model.[121]

*Depsipeptides (**19** and **20**).* Unlike most gelators discussed here, cyclo[CH_2CO-L-leucyl-L-leucine] (**19**, $R_1 = R_2 = CH_2CHMe_2$) is able to gel some polar and apolar liquids like acetonitrile and diethyl ether but is unable to gel the simple alkanes and alcohol (pentanol) investigated. The corresponding cyclo-[CH_2CO-glycylglycine] (**19**, $R_1 = R_2 = H$) is an ineffective gelator.[122] Since the gelator is not soluble in acetonitrile, it is dissolved first in a minimum amount of methanol, water, or dimethyl sulfoxide and then added to the liquid to be gelled. The gels exhibit surprisingly high T_{GS} values. For instance, evaporation of acetone, bp 57 °C, in the gels becomes pronounced only at 85 °C.

The cyclotetrapeptide **20** ($R_1 = R_2 = CHMe_2$) is able to gel water if first dissolved in a very small amount of dimethyl sulfoxide, but the related **20** ($R_1 = CHMe_2$, $R_2 = CH_2CHMe_2$) was able to gel none of the liquids attempted.

Simple Tertiary Amines and Their Quaternary Salts. Small concentrations of some structurally simple tertiary amines and related tertiary and quaternary ammonium halide salts form viscoelastic, thermally reversible gels with organic liquids ranging from dimethyl sulfoxide to dodecane.[123] Optical microscopy and preliminary SANS investigations[124] with some of the gelators have confirmed that the mode of gelation involves a network of strands. All of the gelators have at least two long *n*-alkyl chains attached to nitrogen. Examples of tertiary amines that gel 1-pentanol, for instance, are trioctadecylamine and cholestanyldioctadecylamine. Methyldioctadecylamine does not gel 1-pentanol but does form stable gels with tetramethlytetraphenyltrisiloxane (Dow-Corning 704 silicone oil).[97]

When *N*-methyl-*N*,*N*,*N*-trioctadecylammonium iodide, one of several alkyltrioctadecylammonium halide gelators, is employed, its gels with benzene are stable at room temperature for only hours, but those with dodecane or silicone oil are stable for months (Table 3).[125] By comparison, benzene gels with *N*,*N*,*N*,*N*-tetraoctadecylammonium iodide and with *N*-dodecyl-*N*,*N*,*N*-trioctadecylammonium iodide are stable for weeks and months, respectively. The smaller spherical gelator, *N*,*N*,*N*,*N*-tetradodecylammonium iodide, is more efficient than the octa-

Table 3. Organic Liquids Tested for Gelation with Methyltrioctadecylammonium Iodide

liquid	wt % of gelator	phase	stable period at room temp
cyclohexane	3.7	precipitate[a]	
dodecane	3.0	turbid gel[b]	3 months
hexadecane	2.1	turbid gel[a]	3 months
toluene	4.0	translucent gel[a]	2 h
benzene	4.0	translucent gel[a]	2 h
Dow-Corning 704 silicone oil	2.5	translucent gel[c]	>2 months
1-propanol	4.3	precipitate[a]	
		turbid gel[b]	1 h
1-pentanol	5.0	precipitate[a]	
		turbid gel[b]	4 h
acetonitrile	3.3	precipitate[a]	
dimethyl sulfoxide	2.5	transparent gel[a]	20 min

[a] Cooled from isotropic solution to room temperature (RT) in air. [b] Cooled from isotropic solution in an ice bath. [c] Cooled from isotropic solution to RT after a cosolvent, CH_2Cl_2, was evaporated; the solid could not be dissolved when heated directly in silicone oil.

Table 4. Properties of α-CDOI Gels

liquid	wt % of gelator	phase	stable period[d]
heptane	5.0	*a*	20 h
n-dodecane	5.0	*a*	30 days
	3.0	*a*	30 days
n-hexadecane	5.0	*a*	>1 month
tetramethyltetra-phenyltrisiloxane	3.0	*b*	>12 months
ethanol	4.0	*c*	
1-pentanol	5.0	*c*	
1-nonanol	5.0	*c*	

[a] Translucent gel formed after heating to a temperature which did not result in dissolution of the gelator but led to visual dispersion of it. [b] Transparent gel obtained after a cosolvent (CH_2Cl_2) was evaporated. [c] Solution upon heating; precipitate at RT. [d] Samples kept in sealed glass vials at RT.

Table 5. Properties of β-CDOI Gels

liquid	wt % of gelator	phase	stable period[e]
heptane	5.0	*a*	>12 months
n-octane	5.0	*a*	>50 days
	3.0	*a*	>12 months
n-undecane	5.0	*a*	>12 months
n-dodecane	5.0	*a*	>50 days
	3.0	*a*	
hexadecane	5.0	*a*	>50 days
	3.0	*a*	
tetramethyltetra-phenyltrisiloxane	3.0	*b*	>12 months
ethanol	5.0	*c*	
2/1(v/v) 1-propanol/H_2O	5.0	*c*	
1-pentanol	3.0−5.0	*d*	>12 months
1-nonanol	5.0	*d*	>20 days
	3.0	*d*	12 months
1-decanol	5.0	*d*	>12 months

[a] Translucent gel formed after heating to a temperature which did not result in dissolution of the gelator but led to visual dispersion of it. [b] Transparent gel obtained after a cosolvent (CH_2Cl_2) was evaporated. [c] Solution upon heating; precipitate at RT. [d] Translucent gel slowly formed at RT. [e] Samples kept in sealed glass vials at RT.

decyl analogue with most of the liquids tested. Gelation temperatures do not correlate with the melting points of the neat gelators since solubility limits at higher temperatures play an important role in the initiation of aggregation. Also, the thermotropic liquid-crystalline phases formed by some of the neat gelators[126] may be transient (in somewhat altered forms) in the lyotropic samples and foster aggregation modes leading to strands.

Some quaternary ammonium salts containing a cholestanyl group are also good gelators of liquids like alcohols, alkanes, tetrahydrofuran, and silicone oil.[125] Although 5 wt % of either the α- or β-anomers of *N*-(3-cholestanyl)-*N*,*N*-dimethyl-*N*-octadecylammonium iodide (α- or β-CDOI) gels alkanes, β-CDOI is more efficient and only it is able to gel 1-alkanols (Tables 4 and 5). Low concentrations (<1−3 wt %) of *N*-(3β-cholestanyl)-*N*-methyl-*N*,*N*-dioctadecylammonium iodide (β-CMDI) form very long-lived gels with a wide variety of liquids, ranging from very nonpolar *n*-alkanes to a very polar mixture of 1/2 1-propanol/water (Table 6)! The corresponding chloride (β-CMDCl) can gel fewer liquids for shorter stable periods, and the tertiary ammonium analogue, *N*-(3β-cholestanyl)-*N*,*N*-dioctadecylammonium iodide (β-CDI), was unable to gel any of the liquids tested successfully with β-CMDI. Mesomorphism of the neat salts is clearly not an important factor here since β-CMDI is not liquid-crystalline, but β-CDI forms an enantiotropic smectic phase.

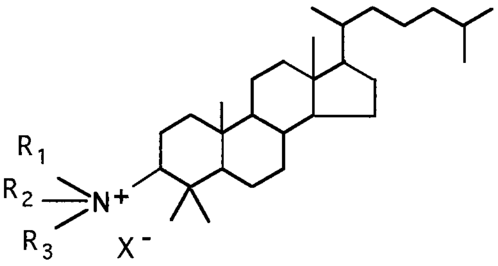

	R1	R2	R3	X
CDOI	Me	Me	$C_{18}H_{37}$	I
CMDI	Me	$C_{18}H_{37}$	$C_{18}H_{37}$	I
CMDCI	Me	$C_{18}H_{37}$	$C_{18}H_{37}$	Cl
CDI	H	$C_{18}H_{37}$	$C_{18}H_{37}$	I

F. Organometallic Compounds

*Mononuclear Copper β-Diketonates (**21**).* Disc-like molecules are shaped favorably to stack and form rodlike aggregates. Examples include 2,3,6,7,10,11-hexapentoxytriphenylene in hexadecane[127] and hexakis(*n*-hexyloxy)triphenylene in dodecane.[128] Complex **21** forms both a neat thermotropic discotic mesophase[129,130] and organogels with *ca.* 99% cyclohexane.[131] The paramagnetic cupric ion allows the gel aggregates to be studied with the X- and Q-bands in EPR spectroscopy. The polar copper diketonate part interacts with neighboring molecules in fibrillar aggregates that rely upon secondary interactions of aromatic substituents, also. The tumbling correlation time, τ, of **21** in the liquid phase was estimated from the hyperfine EPR structure to be *ca.* 4×10^{-10} s. In the gel phase, electron exchange between molecules averages the hyperfine structure, and the frequency dependence of the spectral anisotropy has

Table 6. Properties of β-CMDI Gels

liquid	wt % of gelator	phase	stable period[g]
n-octane	1.0	*a*	>1 month
n-decane	1.0	*a*	15 days
n-dodecane	2.5	*a*	>12 months
	1.0	*a*	>1 month
n-hexadecane	2.5	*a*	>12 months
	1.0	*a*	>1 month
tetrahydrofuran	2.0	*a*	>12 months
tetramethyltetra-phenyltrisiloxane	2.0	*b*	>12 months
methanol	0.8	*c*	6 h
	1.0	*c*	1 day
ethanol	0.8	*c*	6 days
	1.0	*c*	>6 days
1-propanol	1.0	*c*	12 days
1/1(v/v) H_2O/1-propanol	0.9	*c*	9 months
H_2O	2.5	*d*	
1-octanol	3.4	*a*	20 days
	1.0	*e*	
styrene	5.0	*f*	

[a] Translucent gel formed at room temperature (RT). [b] Transparent gel obtained after evaporation of a cosolvent (CH_2Cl_2). [c] Transparent gel formed at room temperature. [d] Gelator insoluble at boiling temperature of liquid. [e] Solution upon heating; precipitate at RT. [f] Solution at RT. [g] Samples kept in sealed glass vials at RT.

been attributed to an increase of τ ($\approx 8 \times 10^{-9}$ s). Evidence for a network of fibers comes from TEM[79] and SANS experiments.[86] The green gel samples exhibit a yield-stress correlated with the existence of (pseudo)crystalline microdomains characterized by Bragg peaks in the WAXS scattering patterns.

*Binuclear Copper Tetracarboxylates (**22**–**24**).* Some disc-like molecules containing metal atoms, such as the binuclear copper tetracarboxylates **22**–**24**, form neat thermotropic columnar mesophases[132–134] and, at <1 wt % concentrations in hydrocarbons, gellike materials.[61,135] The jelly of **22** is a viscoelastic liquid with no significant yield stress or elasticity at zero frequency; it is a "weak gel". The thickening of cyclohexane is characterized by a 150 000-fold increase of the zero shear viscosity at 2 wt % of **22**. SANS experiments demonstrate that aggregates of the bicopper aggregates are rodlike, in very thin semirigid molecular threads (diameter ca. 17 Å for **22**)[61,62,135,136] that have only one molecule within a cross section (Figure 15).

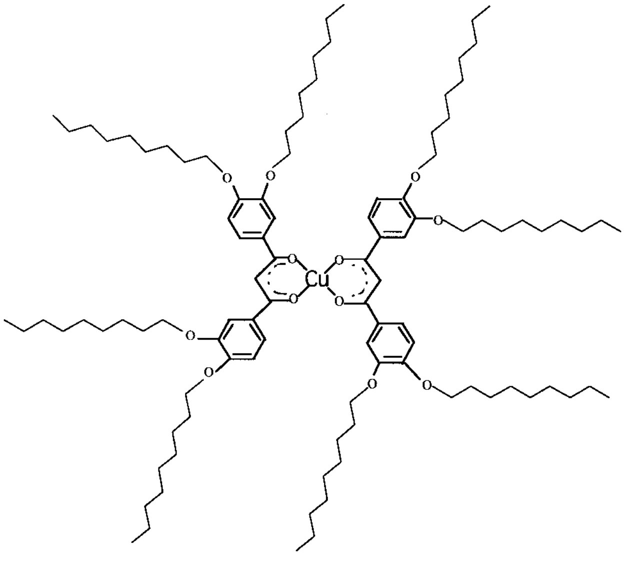

21

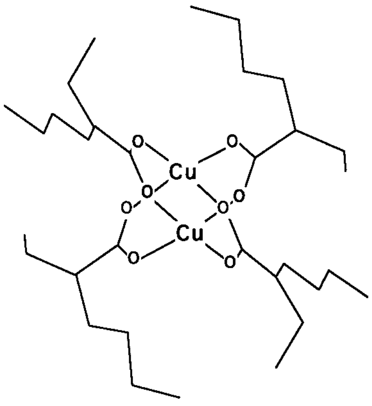

22

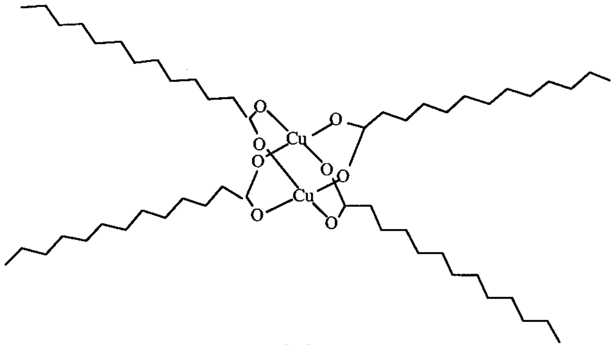

23

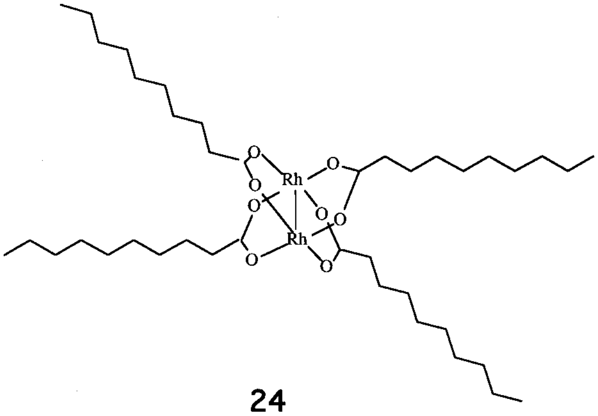

24

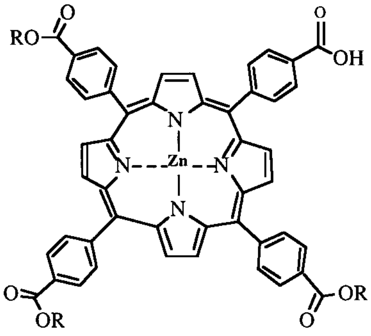

25

Molecules of **22** are connected in stacks through Cu–O coordination bonds, making the symmetry around the copper atoms a deformed octahedron.

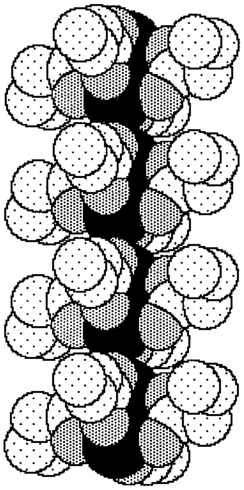

Figure 15. Model of the local structure of the molecular thread formed during aggregation of **22**−**24** in cyclohexane. Atoms: copper (black), oxygen (dark gray), carbon (light gray). The VDW diameter of carbon is 1.57 Å. For the sake of clarity, only the first four C atoms of the alkyl substituent are shown. The chainlike assembly is rigid over distances lower than the persistence length.

Connection sites between neighboring molecules are similar to those found in the crystalline solid (layers with 5.2 Å Cu−Cu interdimer spacing) or in discotic liquid-crystalline phases (crankshaft-like trajectories with 4.7 Å Cu−Cu interdimer spacing). Any change in the two possible connection modes generates curvatures and some flexibility in the chains (Figure 16).[136]

Similar aggregation occurs with analogues of **22** that contain *unbranched*, saturated alkyl groups, but their viscoelastic jellies are metastable and phase separate relatively rapidly. By contrast, the cyclohexane gel of **22** persists for very long periods at room temperature. Possibly, the bulky 2-ethylhexanoate groups of **22** create a steric stress in the molecular stacks that weakens somewhat intermolecular interactions and allows greater chain flexibility.

Within an appropriate concentration range, relaxation of the dynamic shear modulus is approximately monoexponential.[61,62,135−137] The dynamic shear and loss moduli follow roughly the frequency dependencies described by eq 3. A Cole−Cole plot of the dynamic counterpart of the stress relaxation function $G(t)$, $G^*(\omega)$, is a convenient way to categorize viscoelastic Maxwell-type fluids (Figure 17). The corresponding plot of the imaginary part, $G''(\omega)$, as a function of the real part, $G'(\omega)$, gives near semicircles that characterize the degree of monoexponentiality of the stress relaxation.

$$G'(\omega) = G_0\omega^2\tau^2/(1 + \omega^2\tau^2)$$

$$G''(\omega) = G_0\omega\tau/(1 + \omega^2\tau^2) \qquad (3)$$

A model of reversibly breakable polymer-like chains (i.e., "living polymers")[138,60] is consistent with the dynamics of stress relaxation. The assemblies have a thermally equilibrated dynamic molecular weight distribution that is maintained by scission/recombination reactions between molecules in a stack. The dynamics of a chain extremity can be modeled by

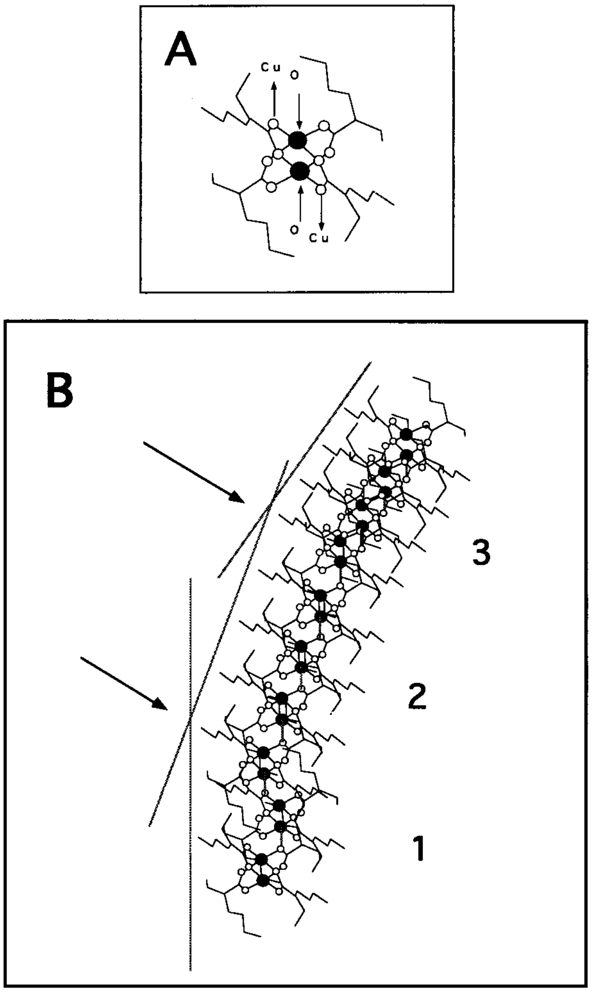

Figure 16. Molecular model of a molecular thread (B) made up of binuclear copper complex molecules (A) connected by copper−oxygen bonds. According to the sequence of connection sites involved, rigid columns or semirigid assemblies with different curvatures can be generated. Arrows indicate a change of the curvature of the aggregate. (Reprinted with permission from ref 136. Copyright 1994 Editrice Compositori.)

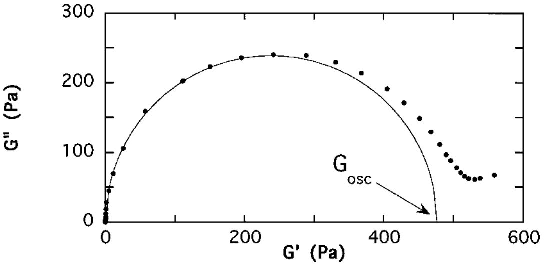

Figure 17. Cole−Cole plot for a viscoelastic solution of **22** (ϕ = 0.71%) in *tert*-butylcyclohexane (●) and the corresponding osculating semicircle (G_{osc}) for pure Maxwellian behavior (-). The increase in G'' in the high-frequency domain is assigned to a more local relaxation process of the chains. (Reprinted with permission from ref 62. Copyright 1994 Editions de Physique.)

reptation theories,[2,139] at least on the time scale of recombination with different chain fragments. They are governed by the lifetime of an aggregate of length L, τ_{break}, and the reptation time of the chain, τ_{rept}. Their relative magnitudes describe the ability of the system to relax through the additional pathway of chain disentanglement, provided by the chain scission reactions. Two extreme situations can be envisioned: (1) almost unbreakable and polydisperse chains, corresponding to $\tau_{\text{break}} >> \tau_{\text{rept}}$, exhibit a stress relaxation proceeding mainly by reptation (or an equivalent process describing the long-time behavior) and, consequently, a stretched exponential relaxation behavior is observed; (2) under conditions where fast scissions are dominant ($\tau_{\text{break}} << \tau_{\text{rept}}$), the lifetime of a chain fragment is very short compared to its relaxation through reptation, and the stress relaxation is characterized by a single exponential decay (a Maxwell liquid).

Scaling of quantities such as the plateau modulus (G_0), the zero shear viscosity (η_0), and the terminal stress relaxation time (τ_0) with the volume fraction (ϕ) is observed over a small concentration range within the semidilute regime. Dynamic and structural information can be obtained from the scaling behavior as well as from the shape of the stress relaxation curve.[140−142] Such procedures have been successfully applied to "living polymers" in aqueous electrolyte solutions.[143,144]

The structure of the aggregates of **22** facilitates the interpretation of some static (or semistatic) and dynamic behavior.[62,136] For example, the scissions appear to occur through reversible reactions of neighboring pairs of molecules rather than via contacts between bent portions of chains. The large elastic modulus values at high frequencies (120 Pa at $\phi = 0.01$ and $\nu = \omega/2\pi = 40$ Hz) of cyclohexane gels of **22** are much larger than those observed for comparable aqueous cetyltrimethylammonium bromide systems due to both the very thin diameter of the molecular threads (and, subsequently, the decreased mesh ξ of the network) and the specific nature of the "cross-links" (i.e., the strength of the interactions, the flexibility of the connecting chains, and their mobility).

Orientational ordering of the aggregates of **22**, as a hexagonal array of rigid columns, is observed in the neat thermotropic discotic mesophase and in the swollen hexagonal and nematic lyotropic phases at concentrations near 50 wt %.[145] In this context, the nodes of the heterogeneous 3D network in dilute gels may be transient swollen nematic microdomains whose spatial extension is restricted by chain flexibility. When the gelator concentration is increased, a topological conflict between the persistence length of the chains and the mesh size of the transient network can occur. Under such conditions, the tightness of the network prevents recombination of different fragments and leads to an apparent (but false) increase of the aggregate lifetime (τ_{break}). This crossover concentration regime, where the spatial correlations become important, may also correspond to a regime where recombinations are diffusion controlled.[146] The chain flexibility can be modified by the type of liquid or alkyl substituent on the gelator, while the energy of chain scission can be changed by the metal type (e.g., to ruthenium[147] or rhodium[145,148]).

*Substituted Metalloporphyrins (**25**) and Related Molecules.* A long-chained ester of *meso*-tetrakis(*p*-carboxyphenyl)porphyrin (**25**),[149] prepared by hydrolysis of one of the four ester groups, forms a thixotropic gellike material in hydrocarbon liquids.[102] Preliminary SAS experiments show that the gelator networks consists of molecular rods.[102] The presence of both the metal and an acidic group appears to be essential for gelation. Changes in the Soret band have been used to study the mechanism of aggregation.[86]

This and preliminary investigations of cationic tetrapyridylporphyrin Cu^{II}, Mn^{II}, and Co^{II} complexes using NMR and EPR techniques[150] are among the few examples of large aggregates being formed by such molecules in organic solvents. Aggregation of metalloporphyrins is a well-known phenomenon in neat thermotropic liquid-crystalline phases[151] and in aqueous solutions.[152] Tetrasubstituted metallo and metal-free phenylporphyrins are known to form a large variety of organized structures.[153,154]

More extensive studies of aggregation of metalloporphyrins in aqueous solutions have been reported since they may be able to mimic proteins and redox systems. For example, a zinc protoporphyrin having two alkylphosphocholine groups (*ca.* 35-Å molecular length) aggregates into fibers of *ca.* 70-Å diameter.[155] A blue-shifted Soret band in the absorption spectrum is attributed to transition dipole interactions of face-to-face stacked porphyrin molecules.[156,157] As mentioned with regard to some other organogelators, studies concerning the solid[158] constitute a valuable basis for analysis of the localized lyotropism of the heterogeneous organogel networks.[159] In this context, systems providing unidirectional assemblies of organometallic arrays, such as coordination polymers[160] or metallomesogens,[161] are expected to contribute to the emerging class of organometallic organogelators.

G. Miscellaneous Types of Gelators

Macrocyclic Gelators. Calix[*n*]arenes ($n = 4-8$) are macrocyclic gelators having long alkanoyl chains (C_m) at the *para* positions of the phenolic rings (see **26** for $n = 8$). They have some conformational flexibility[163] and are frequently utilized in host−guest chemistry[164] and Langmuir monolayer studies.[165,166] As determined by DSC[167,168] or the inverted test-tube method, the T_{SG} of calix[8]arene ($m = 12$) is dependent upon both the liquid type (such as alkanes, carbon disulfide, toluene, and selected alcohols) and gelator concentration. For concentrations in the range $0.02 < \phi < 0.15$, T_{SG} is higher in heptane (35−43 °C) than in cyclohexane (16−27°C), and the slope (dT_{SG}/dC) of the phase diagram is in the order, cyclohexane > hexane > carbon disulfide. Gelation involves the stabilization of stacks of gelator molecules through intermolecular hydrogen bonding of gelator molecules and some gelator/liquid interactions.

Although calix[4]arene ($m = 18$) and calix[8]arene ($m = 12,18$) are gelators, calix[6]arene ($m = 18$) is not. The corresponding noncyclized calixarene analogue with two phenolic rings ($m = 18$) gels only hydrocarbons, while the molecule with only one phenolic ring is not a gelator. These structural features indicate that a minimum number of intermolecular interaction sites per gelator molecule is needed.

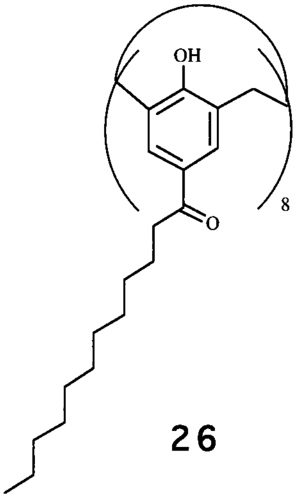

26

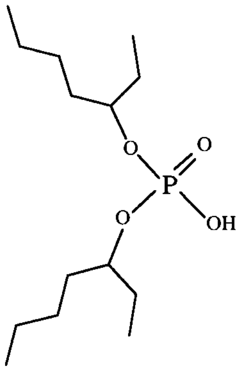

27

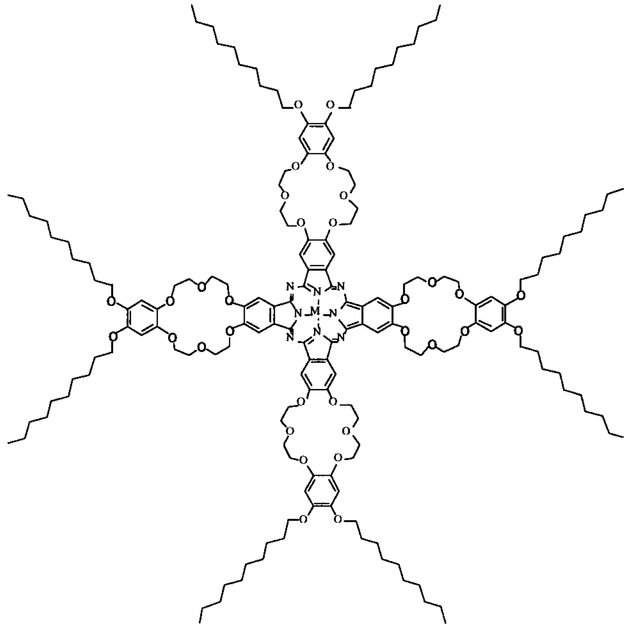

PCC

$F(CF_2)_n(CH_2)_mH$

F_nH_m

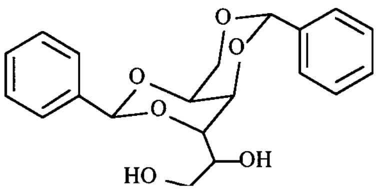

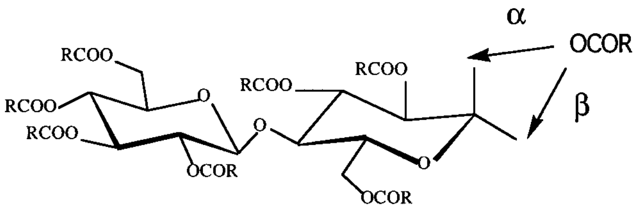

CBO

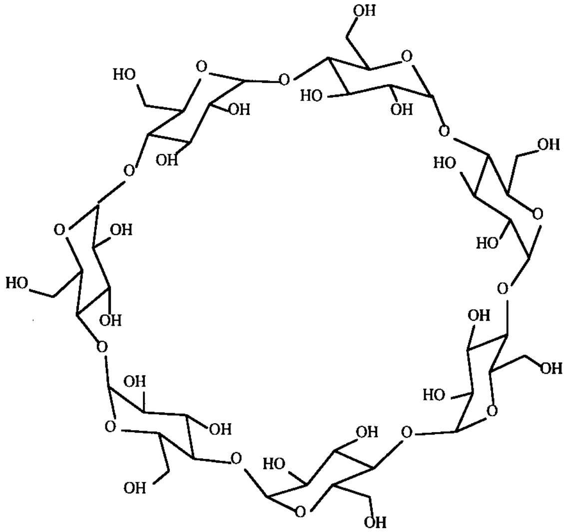

β-CD

There is a preliminary report that 60-crown-20, comprised of 20 ethyleneoxide units, gels acetone and carbon tetrachloride.[169] “Melting” temperatures between 21 and 36 °C were observed when the gelator concentration was 3.5 (the critical concentration, corresponding to $T^* = -3$ °C) to 30 wt %. An interesting gelator of chloroform, tetrakis[4′,5′-bis(decoxy)benzo-18-crown-6]phthalocyanine (**PCC**), has four dibenzo-18-crown-6 moieties symmetrically placed about a phthalocyanine core.[170] The dihydroxysilicon-complexed **PCC** does not act as a gelator, however. Comparison between UV/vis absorption spectra of unaggregated (dilute) and gelled chloroform samples of **PCC** demonstrates that the phthalocyanine groups are stacked in the gel. Transmission electron micrographs of the gels show individual strands with 60-Å diameters and bundles of parallel strands.

Sorbitol and Polyol Derivatives. 1,3:2,4-Di-*O*-benzylidene-D-sorbitol (**DBS**) is a chiral polyol which can gel numerous liquids, varying from hexadecane and dimethyl phthalate to ethanol and ethylene glycol.[171,172] Racemic **DBS** does not form gels. The gelation time, determined by rheological measurements of the storage modulus (G') *vs* time during the sol-to-gel transition,[173] varies with **DBS** concentration in dimethyl phtalate according to a power law with a $^9/_2$ exponent! The kinetics and visual detection of gelation are dependent upon the liquid type. The rigidity of the gels is extremely sensitive to **DBS** concentration; the elastic modulus exhibits a fourth-power dependence on gelator concentration ($G' \approx \phi^4$). Initially clear gels in ethylene glycol[172] with $\phi < 0.15$ are metastable and phase separate. The DSC determined phase diagram with ethylene glycol shows three distinct gelator concentration domains (below $\phi \approx 0.05$, 0.15, and 0.65). Solid-state NMR and freezing-point depression studies confirm the interaction of liquid and **DBS** molecules in the gel.

The relative orientation of the aromatic rings in the aggregates of the gel has been estimated from electronic absorption spectra. A transition from linear (corresponding to a hyperchromic shift) to a parallel stacking (corresponding to a hypochromic shift) occurs at $\phi \approx 0.15$ and is accompanied by an increase of gel crystallinity. By optical microscopy between crossed polarizers, spherulitic textures are observed as extinction crosses (negative optical sign) and rings, suggesting the existence of supramolecular helical arrangements. IR spectra show the presence of hydrogen bonds in the aggregates and UV spectra support a side-by-side aggregation mechanism of the phenyl rings.[174]

*Cellobiose Octa(decanoate) (**CBO**).* Depending upon concentration and temperature, **CBO** in hexadecane forms a lyotropic liquid-crystalline (discotic columnar) phase, micelles, and thermoreversible gels.[175] The latter occurs at <1 wt % of **CBO** and involves a network of strands to immobilize the liquid component. Gelation is relatively slow in samples supercooled below T_{SG}. Both "liquid-crystalline" gel and crystalline gel phases exist over large ranges of compositions.

Partially Fluorinated n-Alkanes ($\mathbf{F_nH_m}$). Partially fluorinated *n*-alkanes ($\mathbf{F_nH_m}$) form birefringent gels with *n*-alkanes when $n = 12$ and $8 < m < 20$. The melting transition proceeds through a gradual disordering, as shown by a broad DSC endotherm.[176,177] Since cyclic alkanes are not gelled, liquid–gelator interactions must be important during the aggregation process.

β-Cyclodextrin (β-CD)/Pyridine Gels. β-Cyclodextrin (β-CD) is a cyclic heptasaccharide of α-1,4 linked glucosidic units that adopts a toroidal shape. Isotropic gels can be formed between anhydrous β-CD and either rigorously dried pyridine[178] or liquids like toluene or chloroform in the presence of small amounts of water.

*Sodium Bis(2-ethylhexyl) Phosphate (**27**) in n-Heptane.* Sodium bis(2-ethylhexyl) phosphate (**27**) in *n*-heptane forms large reverse micelles.[179,180,181] Combined dynamic and static light scattering and viscosimetry measurements show that semiflexible rods grow in the absence of water. This behavior contrasts with the sphere-to-rod transitions of micelles which are promoted by addition of water to systems such as lecithin/isooctane.[182,183] The mean apparent hydrodynamic radius (R_h) and the mean apparent radius of gyration (R_g), when combined with viscosity measurements, enable an estimation of the contour length (L_c) of the aggregates and the related degree of their overlap in the transient network. A molecular packing model has been proposed in which three molecules of **27** lie within a strand cross section. The main driving force for growth of rods is thought to be electrostatic lattice energy, with additional contributions from dipolar and interfacial forces.

H. Two-Component Systems

*Aminopyrimidine (**28a**)/Dialkylbarbituric Acid (**28b**) Mixtures.* Molecules of different structures can form supramolecular structures by association through complementary hydrogen bonds. An ordered supramolecular strand of **28a**/**28b** like that shown in Figure 18 can assemble either in solution or in the solid-state (via cocrystallization).[184] This packing arrangement allows a sorting response and forces a specific orientation of the components in the superstructure.

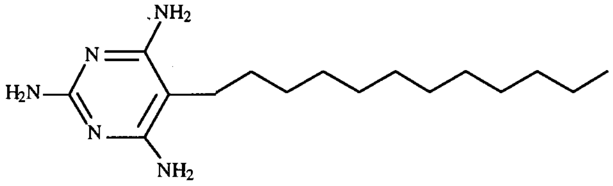

28a

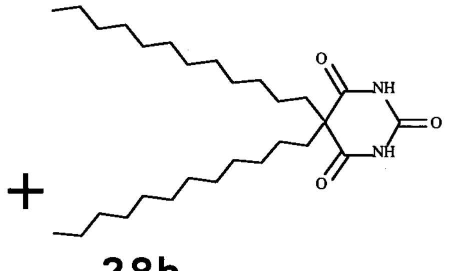

28b

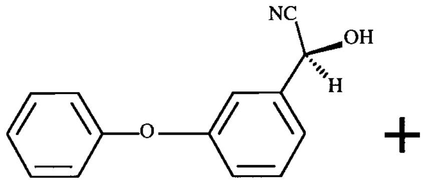

29a

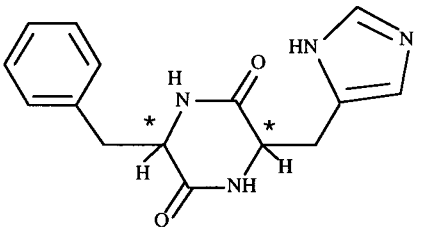

29b

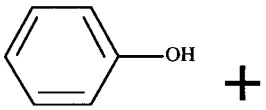

30

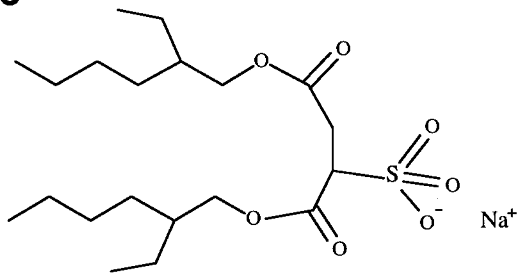

AOT

For example, 1:1 molar mixtures of **28** produce stable organogels in cyclohexane. The minimum concentration of **28** necessary for gelation at 25 °C is ca. 1.1 wt %.[185] FTIR spectra of the related cocrystals confirm the presence of N–H and C=O intermolecular hydrogen bonds.

In the xerogel, a diffraction pattern with four narrow reflections characterizes a layered structure with 19.2-Å separations (smaller than that observed in the related cocrystals).

Another example involves an isocyanuric acid or a triaminopyridine group attached through hexameth-

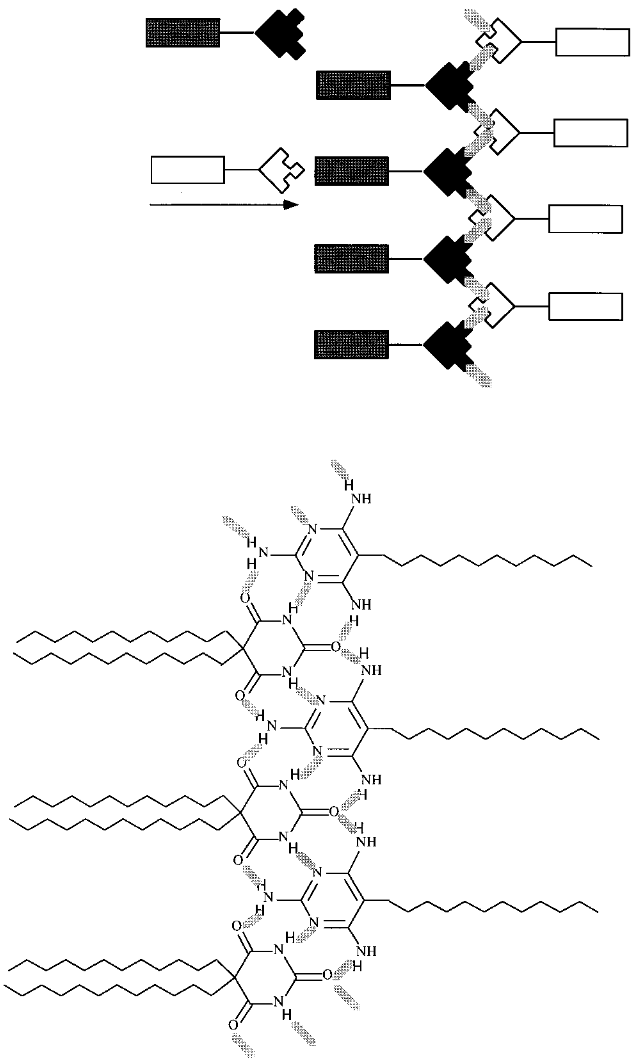

Figure 18. Top: schematic representation of the formation of an ordered supramolecular strand by molecular recognition-induced association of two different molecular units. Each unit contains a group that possesses two identical binding sites complementary to those of the other unit. (Reprinted with permission from ref 184. Copyright 1990 Royal Society of Chemistry.)

ylene linkages to C_3 of cholesterol.[186] Although the isocyanuric acid containing molecule can gel a variety of liquids (via formation of a typical strand network), the triaminopyrimidine analogue cannot. However, 1:1 molar mixtures of the two yield stable gels with a variety of liquids, one of which, methylcyclohexane, cannot be gelled by the isocyanuric acid alone. A model involving tape structures with complementary hydrogen-bonding interactions, like those of the **28** pair, has been advanced to explain the results.

*Phenoxyphenyl- (**29a**)/Cyclo[(R)-phenylalanyl-(R)-histidyl]- (**29b**) Based Molecular Mixtures.* During the asymmetric hydrocyanation of 3-phenoxybenzaldehyde, a gel was obtained with toluene as a consequence of complexation between the two optically active ingredients.[187] Enantioselective complexation was achieved by using a racemic mixture of 2-hydroxy-2-(3-phenoxyphenyl)acetonitrile (in which the *S* enantiomer is complexed) and optically pure cyclo[(*R*)-phenylalanyl-(*R*)-histidyl] in toluene (stereocenters are indicated by * in formula of **29b**).[186]

*Phenol (**30**)/Sodium Bis(2-ethylhexyl) Sulfosuccinate (**AOT**) Mixtures.* The twin-tailed anionic surfactant, **AOT**, is known to self-associate in aqueous and organic solvents.[188,189] A variety of nonpolar liquids have been gelled by a combination of one of several phenols and **AOT** in concentrations below 0.5 wt %![190] Hydrogen bonding between the phenol and the sulfosuccinate head group of **AOT** is essential for gelation; traces of water destroy the gels. Gels do not form with aliphatic alcohols or phenols containing alkyl chains longer than about three carbon atoms. A structural model of the aggregate has been proposed on the basis of broadened phenolic and well-resolved **AOT** and liquid ^{1}H and ^{13}C NMR resonances. The phenolic molecules stack in strands with hydrogen-bonded **AOT** molecules adsorbed on the external surfaces.[191,192]

The pK_a of the phenol and steric hindrance by its *ortho* substituents determine its ability to donate hydrogen bonds to **AOT**.[193] Thus, these parameters are primarily responsible for determining the strength of the gels (as measured by T_{GS}).[193] The liquid influences gel stability based upon its ability to swell **AOT** tails and dissolve both gelator components.

The phenolic molecules decrease the curvature of the interface of reverse **AOT** micelles.[194] This is different from the mode of action of water on aggregates of lecithin in isooctane.[195] Dopants can be incorporated within both parts of the phenol/**AOT** aggregates. Acidic molecules with planar topology can intercalate in the stacked aromatic part, while water is confined to the thin hydrophilic shell.

Ternary Systems with Small Amounts of Water. Complex microemulsions can become gels in which the major component is an alkane. An example is the mixture of **AOT** and 5% aqueous gelatin in 95% isooctane.[196] A proposed model of the gelator network involves micellar percolation and gelatin bridging. The gels are like "frozen" microemulsions where a fluid, gelatin-rich water phase is dispersed in connected water pools within the organic component.[197,198] The conformation of the gelatin polypeptide is a random coil or helical segments depending on its environment and the rate of gelation.

Another example is the transparent, gellike emulsions containing 1 wt % water/surfactant mixtures and 99 wt % hydrocarbon liquid. These metastable gels (exhibiting a static shear modulus and a yield stress) are polyhedral hydrocarbon cells obtained by compression of droplets separated by a continuous flat, aqueous surfactant film.[199] More frequently, an oil-soluble and a water-soluble surfactant are necessary for gelation. Representative examples are mixtures of 2-butanol/water/sodium dodecylsulfate in *n*-hexane[200] or mixtures of a fluorinated neutral amine oxide with a zwitterionic phosphocholine derivative in acyclic or cyclic perfluorohydrocarbons.[201] At ≤50−60% water and surfactant, "gels" (made from spherical microemulsion droplets), which develop "ringing sounds" when the mixtures are mechanically vibrated, can be obtained.[202] Many quaternary systems show gel domains in addition to highly viscous isotropic or anisotropic phases of various structures and compositions. An example is mixtures of sodium dodecylsulfate, butanol, toluene, and water.[203]

Organic solutions of lecithin can become gellike upon addition of a small amount of water.[180] A typical formulation is lecithin ($\phi = 0.14$) and isooctane ($\phi = 0.80$) with *ca.* 3 molecules of water per molecule of lecithin. Numerous complementary techniques have been used to probe the structural, mechanical, and dynamic properties of these systems.[183,204−206] The scaling laws followed by static and dynamic quantities (e.g., zero shear viscosity and hydrodynamic correlation length) demonstrate the existence of an entangled network of long, semirigid, cylindrical reverse micelles. Water induces a sphere-to-rod phase transition and subsequent growth of giant micelles. An analogous example is salted aqueous solutions of cetyltrimethylammonium bromide with polar additives.[207] Variations in the effective area of the aliphatic part of the molecule are important in promoting the transition from spherical to cylindrical curvatures. Much of their behavior is comparable to that of worm-like micelles that exist in complex salted aqueous solutions.[14,208,209] Static and dynamic properties (osmotic compressibility and static and hydrodynamic correlation lengths) of lecithin giant micelles are analogous to semidilute polymer solutions possessing the kinetic features of "living polymers".[60,138,183,210,211] Information concerning the micellar size distribution and intermicellar interactions as a function of concentration can also be gained from analyses of properties in the context of conformational space renormalization group theory.[212]

IV. Applications

Gels have numerous industrial applications due to the great diversity of the structures that they display on microscopic and mesoscopic scales.[213] Their thermoreversibility, chemical sensitivity, and diversity of nanostructures are intrinsic characteristics of organogels which make them excellent candidates for future industrial developments. A brief overview is presented of industrial fields where gels are important, along with the specific properties of these materials and some prospectives for future applications. Several summaries of applications of *polymeric* gels are available.[214−216]

Reverse micellar systems (microemulsions) involving gels find numerous applications in biocatalysis, biomembrane mimetics, extraction processes (universal solvents), and preparation of microparticles.[217] These systems will not be discussed here.

Gels are important in areas such as hydrometallurgy, cosmetics, food processing, and lubrication. Recovery of spilled crude oil or disposal of used cooking oil frequently involves gels or complex microemulsions. Application of organogels in drug delivery can be illustrated with the example of active enzymes and bacteria entrapped in apolar gels of gelatin.[196] Highly concentrated oil-in-water (O/W) emulsions and various gels have been used as aviation fuels and in cosmetics while highly concentrated water-in-oil (W/O) emulsions are used in some explosives technologies. Various complex mixtures of surface-active components (such as cetyl alcohol and polymers) in water and oil are utilized for ointments and creams,[218,219] but their high water content places them outside the scope of this treatise.

Many aqueous gels are employed for macromolecular separations, protein crystallization, etc. Comparable applications, specific to organic fluids, using the properties of hindered transport in pores of the gel networks,[220] may be found in the future. Various applications take advantage of the drag effect, due to steric and hydrodynamic interactions, between permeating macromolecules and the disordered fibrous media. In this context, calix[*n*]arenes are potential membrane filters since they combine molecular pores (between 2.0 Å for calix[4]arene- and 6.4 Å for calix[7]arene-based surfactants)[166] and, in their gelled state, additional nanoscopic pores.

When the liquid is evaporated from a gel, a meniscus develops and the sample shrinks to give a xerogel. Capillary forces and liquid−vapor interfaces are responsible for the collapse of the fragile 3D structure. If a supercritical drying process is used at high temperatures and pressures (i.e., above T_c and P_c), an extremely porous structure, called an aerogel, can be obtained. The remarkable damping of sound and supression of heat transport of some aerogels portends insulation and acoustic applications. Presently, only organometallic oxides (silica) have been utilized to form aerogels,[221] but some organometallic organogelators may serve the same function.

Membranes with aerogel networks, providing small and large diameter holes, may become useful as purification/separation tools. Recently, "reverse aerogels" have been constructed by polymerizing styrene or alkyl methacrylates while gelled by *N*,*N*,*N*,*N*-tetraoctadecylammonium bromide[222] or a gluconamide,[223] and then removing the gelator. These materials, with their networks of microchannels, may be useful as membranes and drug delivery agents.

Gels have been used to produce Turing patterns which result from nonequilibrium self-organization.[224] Such a phenomenon, explained as a spatial symmetry breaking instability, is often important for aspects of morphogenetic developments, even though the role of the gel medium is unclear.[225] The advantages of using gels in place of liquid systems lie in the fact that hydrodynamic convection is reduced and various species can be immobilized. These features are also of importance for slow crystallization of various compounds.[226,227] Reverse micellar systems (microemulsions) find numerous applications in biocatalysis, biomembrane mimetics, extraction processes (universal solvents), and preparation of microparticles.[217]

Gels composed of anisotropic networks and mixed with low molecular mass liquid crystals have been used as active or passive optical components.[228] Anisotropic gels can be easily obtained from organogelators forming rods.[102] They may be of interest for electronic conduction or semiconduction if appropriate donor−acceptor conjugated systems are used.

Studies of the electrical properties of organic solutions of metal soaps, in relationship to the transmission of electric power,[57] have shown that the specific conductance and dielectric loss (ϵ'') reflect the degree of crystallinity and gelation (i.e., heterogeneity) of a sample. Thermotropic liquid crystals have been preferred in the past to lyotropic analogues (due to considerations of energy consumption), but the latter may be of interest in the future.[158,229] Low-dimensional linear systems of stacked organometallic compounds involving phthalocyanine molecules, columnar arrays of cation-radicals of tetrathiafulvalene and selenium analogues, or more complex structures with two-center bridging elements of the metal[230] can exhibit interesting, long-range electronic and magnetic interactions (e.g., molecular-based ferromagnetism) in the condensed solid-state.[231−234]

Some of the gelling systems may be used as temperature or humidity sensors while the ordered microstructures found in their networks can be of interest in templating for materials synthesis.[222,223] Luminescent gels may find applications for linear, anisotropic energy transfer while some chiral organogels can be used for molecular and chiral recognition. Molecular transducers formed by cholesterol-based organogelators[111] which can translate some chiral recognition interactions into readable outputs are promising examples of host−guest signal-responsive chemistry. In such gels, the gel−solution phase transition temperature differentiates the two optical isomers of a monosaccharide (for instance, xylose) added to the gelling system.

Some xerogels of **DBS** are able to act as nucleating agents of polyolefins.[235] These directed polymerizations may lead to high modulus fibers. Some **DBS** derivatives containing ester groups can gel electrolyte solutions for lithium battery applications.[236]

Semiconductor nanostructures are expected from **AOT**/phenol organogels.[192] The growing field of sensors is based upon the detection of specific functionalities by donor−acceptor interactions or detection of morphologies which exploit spatial recognition by cavities, grooves, and channels of the sensor host material;[237] gels offer an attractive medium for new sensor applications. Nanochemistry, which utilizes mostly host systems from solid-state chemistry[238] to yield materials with novel electronic, mechanical, and other properties, may take advantage of specific natures of organogel networks in the future.[239] New gels with low molecular mass organogelators as "intelligent" as their aqueous[240] and polymeric analogues[241−243] may be found.

V. Epilogue

This review has illustrated facets of the fascinating variety of behaviors displayed by organogels. It has attempted to provide as complete answers as are possible today to the three questions presented in the Introduction. None has been answered completely and there is no indication that the foreseeable future will bring an ability to predict whether a specific molecule will gel a selected liquid. To that end, investigations concerning the processes involved in the embryonic stages of gelator nucleation are woefully lacking and are desperately needed. However, given the recent growth of the field, the next few years should bring many additional discoveries of novel gelators, as well as a deeper understanding of the gelation processes.

The authors expect that interest in organogels will increase dramatically in the future. Hopefully, this review will convince readers not to discard gunky looking solutions unless they have recently read the sage dictum of D. Jordon Lloyd,[4] quoted on the first page of this review. Serendipity has been very kind to the authors during their investigations of organogels. May it serve you, also.

VI. Acknowledgments

R.G.W. gratefully acknowledges the U.S. National Science Foundation for its support of the gel research performed at Georgetown. We thank our coauthors cited in the references for their intellectual and physical assistance in deciphering the mysteries of gels.

VII. References

(1) Hoffmann, H. *Adv. Colloid Interface Sci.* **1990**, *32*, 123.
(2) De Gennes, P. G. *Scaling Concepts in Polymer Physics*; Cornell University Press: Ithaca, NY, 1979.
(3) Gelbart, W. M.; Ben-Shaul, A. *J. Phys. Chem.* **1996**, *100*, 13169.
(4) Jordon Lloyd, D. *Colloid Chemistry*; Alexander, J., Ed.; The Chemical Catalog Co.: New York, 1926; Vol. 1, p 767.
(5) Graham, T. *Phil. Trans. Roy. Soc.* **1861**, *151*, 183.
(6) Hermans, P. H. *Colloid Science*; Kruyt, H. R., Ed.; Elsevier: Amsterdam, 1949; Vol. II, p 483.
(7) Flory, P. *J. Discuss Faraday Soc.* **1974**, *57*, 7.
(8) Israelachvili, J. N. *Intermolecular and surface forces*, 3rd ed.; Academic Press: London, 1992; pp 341−435.
(9) Eicke H. F. *Topics in Current chemistry*; Springer-Verlag: Berlin, 1980; Vol. 87, p 91.
(10) Bourrel, M.; Schechter, R. S. *Surfactant Science Series*; Dekker, M.: New York, 1988; Vol. 30, p 111.
(11) Ruckenstein, E.; Nagarajan, R. *J. Phys. Chem.* **1980**, *84*, 1349.
(12) Ekwall, P.; Danielsson, I.; Stenius, P. *Physical Chemistry Series One*; Kerker, M., Ed.; Butterworths: London, 1972; Vol. 7, Chapter 4.
(13) Kitahara, A.; Kon-no, K. *Colloidal dispersions and micellar behavior*; Mittal, K. L., Ed.; ACS Symposium Series; American Chemical Society: Washington, DC, 1975; Chapter 9.
(14) Porte, G.; Appell, J. *J. Phys. Chem.* **1981**, *85*, 2511.
(15) Ferry J. D. *Viscoelastic Properties of Polymers*; Wiley: New York, 1980.
(16) Hermans, P. H. *Colloid Science*; Kruyt, H. R., Ed., Elsevier: Amsterdam, 1969; Vol II.
(17) Russo, P. S. *Reversible polymeric gels and related systems*; Russo, P. S., Ed.; ACS Symposium Series 350; American Chemical Society: Washington, DC, 1987; Chapter 9.
(18) Almdal, K.; Dyre, J.; Hvidt, S.; Kramer, O. *Polym. Gels Networks* **1993**, *1*, 5.
(19) Stauffer, D. *Introduction to percolation*; Taylor and Francis: London, 1985.
(20) Stanley, H. E.; Family, F.; Gould, H. *J. Polym. Sci.: Polym. Symp.* **1985**, *73*, 19.
(21) Stauffer, D.; Coniglio, A.; Adam, M. *Adv. Polym. Sci.* **1982**, *44*, 103.
(22) Burchard, W.; Ross-Murphy, S. B. *Physical Networks, Polymers and Gels*; Elsevier: London, 1990.
(23) Burchard, W.; Stadler, R.; Freitas, L. L.; Möller, M.; Omeis, J.; Mühleisen, E. *Biological and synthetic polymer networks*; Kramer, O., Ed.; Elsevier: London and New York, 1986.
(24) Clark, A.; Ross-Murphy, S. B. *Biopolymers: Adv. Polym. Sci.* Springer-Verlag: Berlin, 1987; Vol. 83, p 57.
(25) Eldridge, J. E.; Ferry, J. D. *J. Phys. Chem.* **1954**, *58*, 992.
(26) Moore, W. J. *Physical Chemistry*, 4th ed.; Prentice Hall: Englewood Cliffs, NJ, 1972.
(27) Murata, K.; Aoki, M.; Suzuki, T.; Harada, T.; Kawabata, H.; Komori, T.; Ohseto, F.; Ueda, K.; Shinkai, S. *J. Am. Chem. Soc.* **1994**, *116*, 6664.
(28) Dubochet, J.; Adrian, M.; Lepault, J.; McDowall, A. *Trends Biochem. Sci.* **1985**, *10*, 143.
(29) Wade, R. H.; Chretien, D. *J. Struct. Biol.* **1993**, *110*, 1.
(30) Clausen, T. M.; Vinson, P. K.; Minter, J. R.; Davis, H. T.; Talmon, Y.; Miller, W. G. *J. Phys. Chem.* **1992**, *96*, 474.
(31) Cabane, C. *Surfactant Solutions, Surfactant Science Series*; Zana, R., Ed.; Marcel Dekker Inc.: New York, 1987; Vol. 22, p 57.
(32) Terech, P. *Croat. Chem. Acta* **1992**, *65 (2)*, 425.
(33) Guinier, A.; Fournet, G. *Small Angle Scattering of X-rays*; Wiley: New York, 1955.

(34) Glatter, O.; Kratky, O. *Small Angle X-ray Scattering*; Academic Press: London, 1982.
(35) Ostuni, E.; Kamaras, P.; Weiss. R. G. *Angew. Chem. Int. Ed. Engl.* **1996**, *35*, 1324.
(36) Candau, S. J. *Light scattering. Surfactant Science Series*; Zana, R., Ed.; Dekker, M.: New York, 1987; p 147.
(37) Muller, M.; Kremer, F.; Stadler, R.; Fisher, E. W.; Seidel, U. *Colloid Polym. Sci.* **1995**, *273*, 38.
(38) Aliotta, F.; Fontanella, M. E.; Galli, G.; Lanza, M.; Migliardo, P.; Salvato, G. *J. Phys. Chem.* **1993**, *97*, 733.
(39) Mezei, F. *Physics, Neutron Spin Echo*; Springer-Verlag: Berlin, 1980; Vol. 128, p 3.
(40) Polishuk, A. T. *J. Am. Soc. Lubn. Eng.* **1977**, *33*, 133.
(41) Uzu, Y. *J. Jpn. Oil Chem. Soc.* **1975**, *24*, 261.
(42) Fiero, G. W. *J. Am. Pharm. Assoc.* **1940**, *29*, 502.
(43) Boner, C. J. *Manufacture and Application of Lubricating Greases*; Reinhold Publishing Corp.: New York, 1960.
(44) Georges J. M. *Tribology Series*; Elsevier: Amsterdam, 1982; Vol. 7, p 651.
(45) Mansot, J. L.; Terech, P.; Martin, J. M. *Colloids Surf.* **1989**, *39*, 321.
(46) Sakamoto, K.; Yoshida, R.; Hatano, M.; Tachibana, T. *J. Am. Chem. Soc.* **1978**, *100 (22)*, 6898.
(47) Tachibana, T.; Mori, T.; Hori, K. *Bull. Chem. Soc. Jpn.* **1980**, *53*, 1714; **1981**, *54*, 73.
(48) Terech, P. *Colloid Polym. Sci.* **1991**, *269*, 490.
(49) Terech, P.; Rodriguez, V.; Barnes, J. D.; McKenna, G. B. *Langmuir* **1994**, *10*, 3406.
(50) Tachibana, T.; Mori, T.; Hori, K. *Nature* **1979**, *278*, 578.
(51) Tachibana, T.; Kitazawa, S.; Takeno, H. *Bull. Chem. Soc. Jpn.* **1970**, *43*, 2418.
(52) Terech, P.; Wade, R. H. *J. Colloid Interface Sci.* **1988**, *125 (2)*, 542.
(53) Tachibana, T.; Hori, K. *J. Colloid Interface Sci.* **1977**, *61 (2)*, 398.
(54) Fuhrhop, J-H.; Schnieder, P.; Rosenberg, J.; Boekema, E. *J. Am. Chem. Soc.* **1987**, *109 (11)*, 3387.
(55) Snijder, C. S.; de Jong, J. C.; Meetsma, A.; van Bolhuis, F.; Feringa, B. L. *Chem. Eur. J.* **1995**, *1*, 594.
(56) Kaneko, F.; Shirai, O.; Miyamoto, H.; Kobayashi, M.; Suzuki, M. *J. Phys. Chem.* **1994**, *98*, 2185.
(57) Pilpel, N. *Chem. Rev.* **1963**, *63*, 221.
(58) Gaskins, F. H.; Brodnyan, J. G.; Philippoff, W. *Trans. Soc. Rheol.* **1969**, *13 (1)*, 17.
(59) Leibler, L.; Rubinstein, M.; Colby, R. H. *Macromolecules* **1991**, *24*, 4701.
(60) Cates, M. E. *Macromolecules* **1987**, *20*, 2289.
(61) Terech, P.; Schaffhauser, V.; Maldivi, P.; Guenet, J. M. *Europhys. Lett.* **1992**, *17*, 515.
(62) Terech, P.; Maldivi, P.; Dammer, C. *J. Phys. II Fr.* **1994**, *4*, 1799.
(63) Zhou, Z.; Georgalis, Y.; Liang, W.; Li J.; Xu, R.; Chu, B. *J. Colloid Interface Sci.* **1987**, *116 (2)*, 473.
(64) Fukasawa, J-I; Tsutsumi, H. *J. Colloid Interface Sci.* **1991**, *143 (1)*, 69.
(65) Klyne, W. *The Chemistry of Steroids*; Wiley: New York, 1960.
(66) Ramanathan, N.; Currie, A. L.; Ross Colvin, J. *Nature* **1961**, *4778*, 779.
(67) Hoffmann, S. *Mol. Cryst. Liq. Cryst.* **1984**, *110*, 277.
(68) Toyne, K. J. *Critical Reports on Applied Chemistry;* Gray, G. W., Ed.; Wiley: Chichester, 1987; Vol. 22, pp 28, 131 and references cited therein.
(69) Technical Bulletin from Nikko Chemicals Co., Ltd., 1-4-8 Nihonbashi-Bakurocho, Japan, 1989.
(70) Bujanowski, V. J.; Katsoulis, D. E.; Ziemelis, M. J. *J. Mater. Chem.* **1994**, *4*, 1181.
(71) Martin-Borret, O.; Ramasseul, R.; Rassat, R. *Bull. Soc. Chim. Fr.* **1979**, *7−8*, II-401.
(72) Terech, P.; Ramasseul, R.; Volino, F. *J. Colloid Interface Sci.* **1983**, *91 (1)*, 280.
(73) Freed, J. H. *Spin Labelling: Theory and Applications*; Berliner, L., Ed.; Academic Press: New York, 1976; Chapter 3.
(74) Terech, P. *J. Colloid Interface Sci.* **1985**, *107 (1)*, 244.
(75) Avrami, M. *J. Chem. Phys.* **1939**, *7*, 1103; **1940**, *II8*, 212; **1941**, *III9*, 177.
(76) Terech, P.; Ramasseul, R.; Volino, F. *J. Phys. Fr.* **1985**, *46*, 895.
(77) Wade, R. H.; Terech, P.; Hewat, E. A.; Ramasseul, R.; Volino, F. *J. Colloid Interface Sci.* **1986**, *114 (2)*, 442.
(78) Terech, P. *Reversible polymeric gels and related systems*; Russo, P. S., Ed.; ACS Symposium Series 350; American Chemical Society: Washington, DC, 1987; Chapter 9.
(79) Terech, P. *The living cell in four dimensions*; Paillotin, G., Ed.; American Institute of Physics Conference Proceedings, 1991; Vol. 226, p 518.
(80) Pfannemüller, B.; Welte, W. *Chem. Phys. Lipids* **1985**, *37 (2)*, 227.
(81) Terech, P.; Berthet, C. *J. Phys. Chem.* **1988**, *92*, 4269.
(82) Terech, P. *J. Surface Sci. Technol.* **1989**, *5 (2)*, 163.
(83) Terech, P. *Mol. Cryst. Liq. Cryst.* **1989**, *166*, 29.
(84) Terech, P.; Rodriguez, V. *Progr. Colloid Polym. Sci.* **1994**, *97*, 151.
(85) Terech, P. *J. Phys. Fr.* **1989**, *50*, 1967.
(86) Terech, P., unpublished data.
(87) Brotin, T.; Utermöhlen, R.; Fages, F.; Bouas-Laurent, H.; Desvergne, J. P. *J. Chem. Soc., Chem. Commun.* **1991**, 416.
(88) Bouas-Laurent, H.; Desvergne, J. P. *Photochromism, Molecules and Systems*; Dürr, H., Bouas-Laurent, H., Eds.; Elsevier: Amsterdam, 1990; p 561.
(89) Brotin, T.; Desvergne, J. P.; Fages, F.; Utermöhlen, R.; Bonneau, R.; Bouas-Laurent, H. *Photochem. Photobiol.* **1992**, *55 (3)*, 349.
(90) Terech, P; Desvergnes, J. P.; Bouas-Laurent, H. *J. Colloid Interface Sci.* **1995**, *174*, 258.
(91) Ladd, M. F. C.; Palmer, R. A. *Structure determination by X-ray Crystallography*; Plenum Press: New York, 1985.
(92) Lin, Y-c; Weiss, R. G. *Macromolecules* **1987**, *20*, 414.
(93) Itoh, T.; Katsoulis, D. E.; Mita, I. *J. Mater. Chem.* **1993**, *3(12)*, 1303.
(94) Smith, J. M.; Katsoulis, D. E. *J. Mater. Chem.* **1995**, *5*, 1899.
(95) Mukkamala, R.; Weiss, R. G. *J. Chem. Soc., Chem. Commun.* **1995**, 375.
(96) Lin, Y-c.; Kachar, B.; Weiss, R. G. *J. Am. Chem. Soc.* **1989**, *111*, 5542.
(97) Lu, L. Ph. D. Thesis, Georgetown University, Washington, DC, 1997.
(98) Furman, I.; Weiss, R. G. *Langmuir* **1993**, *9*, 2084.
(99) Demus, D.; Richter, L. *Textures of Liquid Crystals*; Verlag Chemie: Veinheim, 1978.
(100) Lin, Y-c.; Weiss, R. G. *Liquid Crystals* **1989**, *4 (4)*, 367.
(101) Mewis, J. *J. Non-Newtonian Fluid Mechanics* **1979**, *6*, 1.
(102) Terech, P.; Gebel, G.; Ramasseul, R., *Langmuir* **1996**, *12*, 4321.
(103) Ostuni, E. M. S. Thesis; Georgetown University, Washington, DC, 1995.
(104) Terech, P.; Furman, I.; Weiss, R. G. *J. Phys. Chem.* **1995**, *99*, 9558.
(105) Terech, P.; Ostuni, E.; Weiss, R. G. *J. Phys. Chem.* **1996**, *100*, 3759.
(106) Terech, P.; Furman, I.; Bouas-Laurent, H.; Desvergne, J. P.; Ramasseul, R.; Weiss, R. G. *J. Chem. Soc., Faraday Discuss.* **1995**, *101*, 345.
(107) Mukkamala, R.; Weiss, R. G. *Langmuir* **1996**,*12*,1474.
(108) Murata, K.; Aoki, M.; Susuki, T.; Harada, T.; Kawabata, H.; Komori, T.; Ohseto, F.; Ueda, K.; Shinkai, S. *J. Am. Chem. Soc.* **1994**, *116*, 6664.
(109) Terech, P. *Liquid Cryst.* **1991**, *9 (1)*, 59.
(110) Kawabata, H.; Murata, K.; Harada, T.; Shinkai, S. *Langmuir* **1995**, *11*, 623.
(111) James, T. D.; Kawabata, H.; Ludwig, R.; Murata, K.; Shinkai, S. *Tetrahedron* **1995**, *51 (2)*, 555.
(112) Campbell, J.; Kuzma, M.; Labes, M. *Mol. Cryst. Liq. Cryst.* **1983**, *95*, 45.
(113) Yasuda, Y.; Iishi, E.; Inada, H.; Shirota, Y. *Chem. Lett.* **1996**, 575.
(114) Hanabusa, K.; Okui, K.; Karaki, K.; Koyama, T.; Shirai, H. *J. Chem. Soc., Chem. Commun.* **1992**, 1371.
(115) Hanabusa, K.; Tange, J.; Taguchi, Y.; Koyama, T.; Shirai, H. *J. Chem. Soc., Chem. Commun.* **1993**, 390.
(116) Hikada, S.; Murata, M.; Onai. T. *J. Chem. Soc., Chem. Commun.* **1984**, 562.
(117) Fuhrhop, J-H.; Schnieder, P.; Boekema, E.; Helfrich, W. *J. Am. Chem. Soc.* **1988**, *110*, 2861.
(118) Fuhrhop, J-H.; Demoulin, C.; Rosenberg, J.; Boettcher, C. *J. Am. Chem. Soc.* **1990**, *112*, 2827.
(119) Hanabusa, K.; Naka, Y.; Koyama, T.; Shirai, H. *J. Chem. Soc., Chem. Commun.* **1994**, 2683.
(120) Menger, F. M.; Venkatasubban, K. S. *J. Org. Chem.* **1978**, *43*, 3413.
(121) Hanabusa, K.; Matsumoto, Y.; Miki, T.; Koyama, T.; Shirai, H. *J. Chem. Soc., Chem. Commun.* **1994**, 1401.
(122) de Vries, E. J.; Kellogg, R. M. *J. Chem. Soc., Chem. Commun.* **1993**, 238.
(123) Lu, L.; Weiss, R. G. *Langmuir* **1995**, *11*, 3630.
(124) Schurr, O.; Glinka, C.; Weiss, R. G., unpublished results.
(125) Lu, L.; Weiss, R. G. *J. Chem. Soc. Chem. Commun.* **1996**, 2029.
(126) Lu, L.; Nagana Gowda, G. A.; Khetrapal, C. L.; Weiss, R. G. *Liq. Cryst.* **1997**, *22*, 23.
(127) Sheu, E. Y.; Liang, K. S.; Chiang, L. Y. *J. Phys. Fr.* **1989**, *50*, 1279.
(128) Gallivan, J. P.; Schuster, G. B. *J. Org. Chem.* **1995**, *60*, 2423.
(129) Godquin-Giroud, A. M. *J. Phys. Lett.* **1984**, *45*, L-387.
(130) Godquin-Giroud, A. M.; Gauthier, M. M.; Sigaud, G.; Hardouin, F.; Achard, F. *Mol. Cryst. Liq. Cryst.* **1986**, *132*, 35.
(131) Terech, P.; Chachaty, C.; Gaillard, J.; Godquin-Giroud, A. M. *J. Phys. Fr.* **1987**, *48*, 663.
(132) Godquin-Giroud, A. M.; Marchon, J. C. *J. Phys. Lett.* **1984**, *45*, L-681.
(133) Attard, G. S.; Cullum, P. R. *Liq. Cryst.* **1990**, *8 (3)*, 299.
(134) Abied, H.; Guillon, D.; Skoulios, A.; Weber, P.; Godquin-Giroud, A. M.; Marchon, J. C. *Liq. Cryst.* **1987**, *2*, 269.
(135) Terech, P.; Schaffhauser, V.; Maldivi, P.; Guenet, J. M. *Langmuir* **1992**, *8*, 2104.
(136) Terech, P. *Nuovo Cimento* **1994**, *16D (7)*, 757.

(137) Dammer, C.; Maldivi, P.; Terech, P.; Guenet, J. *Langmuir* **1995**, *11*, 1500.
(138) Cates, M. E. *J. Phys. Fr.* **1988**, *49*, 1593.
(139) Doi M.; Edwards S. F. *The Theory of Polymer Dynamics*; Clarendon: Oxford, 1986.
(140) Turner, M. S.; Cates, M. E. *Langmuir* **1991**, *7*, 1590.
(141) Turner, M. S.; Cates, M. E. *J. Phys. II Fr.* **1992**, *2*, 503.
(142) Granek, R.; Cates, M. E. *J. Chem. Phys.* **1992**, *96 (6)*, 4758.
(143) Kern, F.; Zana, R.; Candau, S. J. *Langmuir* **1991**, *7*, 1344.
(144) Berret, J. F.; Appell, J.; Porte, G. *Langmuir* **1993**, *9*, 2851.
(145) Ibn-Elhaj, M.; Guillon, D.; Skoulios, A.; Godquin-Giroud, A. M.; Marchon, J. C. *J. Phys. II Fr.* **1992**, *2*, 2197.
(146) O'Shaughnessy, B.; Yu, J. *Phys. Rev. Lett.* **1995**, *74 (21)*, 4329.
(147) Bonnet, L.; Cukiernik, F. D.; Maldivi, P.; Godquin-Giroud, A. M.; Marchon, J. C. *Chem. Mater.* **1994**, *6*, 31.
(148) Marchon, J. C.; Maldivi, P.; Godquin-Giroud A. M.; Guillon, D.; Skoulios, A.; Strommen, D. P. *Philos. Trans. R. Soc. London* **1990**, *A330*, 109.
(149) Ramasseul, R.; Maldivi, P.; Marchon, J. C. *Liquid Crystals* **1993**, *13 (5)*, 729.
(150) Yamamura, T. *Chem. Lett.* **1977**, 773.
(151) Bruce, D. W.; Wali, M. A.; Qing Min Wang *J. Chem. Soc., Chem. Commun.* **1994**, 2089.
(152) Fuhrhop, J-H.; Bindig, U.; Siggel, U. *J. Chem. Soc., Chem. Commun.* **1994**, 1583.
(153) Byrn, M. P.; Curtis, C. J.; Khan, S. I.; Sawin, P. A.; Tsurumi, R.; Strouse, C. E. *J. Am. Chem. Soc.* **1990**, *112*, 1865.
(154) Byrn, M. P.; Curtis, C. J.; Hsiou, Y.; Khan, S. I.; Sawin, P. A.; Tendick, S. K.; Terzis, A.; Strouse, C. E. *J. Am. Chem. Soc.* **1993**, *115*, 9480.
(155) Tsuchida, E.; Komatsu, T.; Toyano, N.; Kumamoto, S.; Nishide, H. *J. Chem.. Soc., Chem. Commun.* 1993, 1731.
(156) Dolphin, D. *The porphyrins*, Physical Chemistry, Part A; Academic Press: New York, 1978; Vol. III.
(157) Fuhrhop, J.-H.; Demoulin, C.; Boettcher, C.; Köning, J.; Siggel, U. *J. Am. Chem. Soc.* **1992**, *114*, 4159.
(158) Hanack, M.; Lang, M. *Adv. Mater.* **1994**, *6 (11)*, 819.
(159) Simon, J.; Sirlin, C. *Pure Appl. Chem.* **1989**, *61*, 1625.
(160) Loeb, S. J.; Shimizu, G. K. H. *J. Chem. Soc., Chem. Commun.* **1993**, 1395.
(161) Godquin-Giroud, A. M.; Maitlis, P. M. *Angew. Chem. Int. Ed. Engl.* **1991**, *30*, 375.
(162) Chandrasekhar, S.; Ranganath, G. S. *Rep. Prog. Phys.* **1990**, *53*, 57.
(163) Gutsche, C. D.; Bauer, L. J. *J. Am. Chem. Soc.* **1985**, *107*, 6052, 6059.
(164) Gutsche, C. D.; Bauer, L. J. *J. Am. Chem. Soc.* **1985**, *107*, 6063.
(165) Dedek, P.; Webber, A. S.; Janout, V.; Hendel, R. A.; Regen, S. L. *Langmuir* **1994**, *10*, 3943.
(166) Markowitz, M. A.; Janout, V.; Castner, D. G.; Regen, S. L. *J. Am. Chem. Soc.* **1989**, *111*, 8192.
(167) Aoki, M.; Murata, K.; Shinkai, S. *Chem. Lett.* **1991**, 1715.
(168) Aoki, M.; Nakashima, K.; Kawabata, H.; Tsutsui, S.; Shinkai, S. *J. Chem. Soc., Perkin Trans 2* **1993**, 347.
(169) Prasad, A.; Marand, H.; Bheda, M.; Gibson, H. W. *Polym. Prepr.* **1991**, *32*, 469.
(170) van Nostrum, C. F.; Picken, S.; Schouten, A.-J.; J. Nolte, R. J. M. *J. Am. Chem. Soc.* **1995**, *117*, 9957.
(171) Yamasaki, S.; Tsutsumi, H. *Bull. Chem. Soc. Jpn.* **1994**, *67*, 2053.
(172) Yamasaki, S.; Tsutsumi, H. *Bull. Chem. Soc. Jpn.* **1994**, *67*, 906.
(173) McKenna, G. B.; Kern, F.; Candau, S. J. *Polymer Prepr.* **1991**, *32*, 455.
(174) Yamasaki, S.; Ohashi, Y.; Tsutsumi, H.; Tsujii, K. *Bull. Chem. Soc. Jpn.* **1995**, *68*, 146.
(175) Ide, N.; Fukuda, T.; Miyamoto, T. *Bull. Chem. Soc. Jpn.* **1995**, *68*, 3423.
(176) Twieg, R. J.; Russell, T. P.; Siemens, R.; Rabolt, J. F. *Macromolecules* **1985**, *18*, 1361.
(177) Rabolt, J. F.; Russell, T. P.; Siemens, R.; Twieg, R. J.; Farmer, B. *Polym. Prepr.* **1991**, *32*, 223.
(178) De Rango, C.; Charpin, P.; Navaza, J.; Keller, N.; Nicolis, I.; Villain, F.; Coleman, A. W. *J. Am. Chem. Soc.* **1992**, *114*, 5475.
(179) Yu, Z-J.; Zhou, N-F.; Neuman, R. D. *Langmuir* **1992**, *8*, 1885.
(180) Yu, Z-J.; Neuman, R. D. *Langmuir* **1994**, *10*, 2553.
(181) Bhattacharyya, S. N.; Ganguly, B. *J. Colloid Interface Sci.* **1987**, *118 (1)*, 15.
(182) Luisi, P. L.; Scartazzini, R.; Haering, G.; Schurtenberger, P. *Colloid Polym. Sci.* **1990**, *268*, 356.
(183) Schurtenberger, P.; Scartazzini, R.; Luisi, P. L. *Rheol. Acta* **1989**, *28*, 372.
(184) Lehn, J.-M.; Mascal, M.; DeCian, A.; Fisher, J. *J. Chem. Soc., Chem. Commun.* **1990**, 479.
(185) Hanabusa, K.; Miki, T.; Taguchi, Y.; Koyama, T.; Shirai, H. *J. Chem. Soc., Chem. Commun.* **1993**, 1382.
(186) Jeong, S. W.; Murata, K.; Shinkai, S. *Supramolec. Sci.* **1996**, *3*, 83.
(187) Danda, H.; Nishikawa, H.; Otaka, K. *J. Org. Chem.* **1991**, *56*, 6740.
(188) Mukherjee, K.; Moulik, S. P. *Langmuir* **1993**, *9*, 1727.
(189) Peri, J. B. *J. Colloid Interface Sci.* **1969**, *29 (1)*, 6.
(190) Xu, X.; Ayyagari, M.; Tata, M.; John, V. T.; McPherson, G. L. *J. Phys. Chem.* **1993**, *97*, 11350.
(191) Tata, M.; John, V. T.; Waguespack, Y. Y.; McPherson, C. L. *J. Am. Chem. Soc.* **1994**, *116*, 9464.
(192) Tata, M.; John V. T.; Waguespack Y. Y.; McPherson G. L. *J. Phys. Chem.* **1994**, *98*, 3809.
(193) Magid, L. J.; Kon-no, K.; Martin, C. A. *J. Phys. Chem.* **1981**, *85*, 1434.
(194) Rao, A. M.; John, V. T.; Gonzalez, R. D.; Akkara, J. A.; Kaplan, D. A. *Biotechnol. Bioeng.* **1993**, *41*, 531.
(195) Capitani, D.; Segre, A. L.; Sarapani, R. *Langmuir* **1991**, *7*, 250.
(196) Haering, G.; Luisi, P. L. *J. Phys. Chem.* **1986**, *90*, 5892.
(197) Quellet, C.; Eicke, H-F. *Chimia* **1986**, *40 (7−8)*, 233.
(198) Quellet, C.; Eicke, H-F.; Sager, W. *J. Phys. Chem.* **1991**, *95*, 5642.
(199) Bergeron, V.; Sebba, F. *Langmuir* **1987**, *3*, 857. Comments by Princen, H. M. *Langmuir* **1988**, *4 (2)*, 486.
(200) Ebert, G.; Platz, G.; Rehage, H. *Ber. Bunsenges. Phys. Chem.* **1988**, *92*, 1158.
(201) Krafft, M.-P.; Riess, J. G. *Angew. Chem. Int. Engl.* **1994**, *33 (10)*, 1100.
(202) Gradzielski, M.; Hoffmann, H.; Oetter, G. *Colloid Polym. Sci.* **1990**, *268*, 167.
(203) Hirsch, E.; Wittmann, J. C.; Candau, F. *J. Dispersion Sci. Technol.* **1982**, *3 (4)*, 351.
(204) Scartazzini, R.; Luisi, P. L. *J. Phys. Chem.* **1988**, *92*, 829.
(205) Schurtenberger, P.; Scartazzini, R.; Magid, L. J.; Leser, M. E.; Luisi, P. L. *J. Phys. Chem.* **1990**, *94*, 3695.
(206) Schurtenberger, P.; Magid, L. J.; King, S. M.; Lindner, P. *J. Phys. Chem.* **1991**, *95(11)*, 4173.
(207) Lin, Z.; Cai, J. J.; Scriven, L. E.; Davis, H. T. *J. Phys. Chem.* **1994**, *98*, 5984.
(208) Candau, S. J. *J. Phys. Fr.* **1990**, *51*, 977.
(209) Rehage, H.; Hoffmann, H. *J. Phys. Chem.* **1988**, *92*, 4712.
(210) Cates, M. E.; Candau, S. J. *J. Phys.: Condens. Matter* **1990**, *2*, 6869.
(211) Schurtenberger, P.; Cavaco, C. *Langmuir* **1994**, *10*, 100.
(212) Schurtenberger, P.; Cavaco, C. *J. Phys. II Fr.* **1993**, *3*, 1279.
(213) Prost, J.; Rondelez, F. *Nature* **1991**, *350*, 11.
(214) Dickinson, E., Ed.; *Food Polymers, Gels and Colloids*; The Royal Society of Chemistry: Cambridge, 1991.
(215) Russo, P. S., Ed.; *Reversible Polymeric Gels and Related Systems*; American Chemical Society: Washington, DC, 1987.
(216) Guenet, J.-M. *Thermoreversible Gelation of Polymers and Biopolymers*; Academic Press: London, 1992.
(217) Rees, G. D.; Robinson, B. H. *Adv. Mater.* **1993**, *5 (9)*, 608.
(218) De Vringer, T.; Joosten, J. G. H.; Junginger, H. E. *Colloid Polym. Sci.* **1987**, *265*, 167.
(219) Patel, H. K.; Rowe, R. C.; McMahon, J.; Stewart, R. F. *Int. J. Pharm.* **1985**, *25*, 13.
(220) Phillips, R. J.; Deen, W. M.; Brady, J. F. *J. Colloid Interface Sci.* **1990**, *139*, 363.
(221) (a) Fricke, J.; Emmerling A. *Adv. Mater.* **1991**, *3 (10)*, 504. (b) Fajnor, V. S.; Jesenak, K. *Chem. Listy* **1994**, *88 (1)*, 24.
(222) Gu, W.; Lu, L.; Chapman, G. B.; Weiss, R. G. *J. Chem. Soc., Chem. Commun.* **1997**, 543.
(223) Hafkamp, R. J. H.; Kokke, P. A.; Danke, I. M.; Guerts, H. P. M.; Rowan, A. E.; Feiters, M. C.; Nolte, R. J. M. *J. Chem. Soc., Chem. Commun.* **1997**, 545.
(224) Yamaguchi, T.; Kuhnert, L.; Nagy-Ungvarai, Zs; Müller, S. C.; Hess, B. *J. Phys. Chem.* **1991**, *95*, 5831.
(225) Agladze, K.; Dulos, E.; De Kepper, P. *J. Phys. Chem.* **1992**, *96*, 2400.
(226) Andreazza, P.; Lefaucheux, F.; Mutaftschiev, B. *J. Cryst. Growth* **1988**, *92*, 415.
(227) Robert, M. C.; Lefaucheux, F. *J. Crystal Growth* **1988**, *90*, 358.
(228) Rifat, A.; Hikmet, A. M. *Adv. Mater.* **1992**, *4 (10)* 679.
(229) Piechocki, C.; Simon, J.; Skoulios, A.; Guillon, D.; Weber, P. *J. Am. Chem. Soc.* **1982**, *104*, 5245.
(230) Rosenblum, M. *Adv. Mater.* **1994**, *6 (2)*, 159.
(231) Weber, P.; Guillon, D.; Skoulios, A. *J. Phys. Chem.* **1987**, *87*, 2242.
(232) Albouy, P. A. *J. Phys. Chem.* **1994**, *98*, 8543.
(233) Ricco, M.; Dalcanale, E. *J. Phys. Chem.* **1994**, *98*, 9002.
(234) Imahori, H.; Higuchi, H.; Matsuda, Y.; Itagaki, A.; Sakai, Y.; Ojima, J.; Sakata, Y. *Bull. Chem. Soc. Jpn.* **1994**, *67*, 2500.
(235) Thierry, A.; Straupe, C.; Lotz, B.; Wittmann, J. C. *Polymer Commun.* **1990**, *31*, 299.
(236) Ue, M.; Kaitoh, M.; Yazsukawa, E.; Mori, S. *Electrochim. Acta* **1993**, *38 (9)*, 1301.
(237) Dickert, F. L.; Haunschild, A. *Adv. Mater.* **1993**, *5 (12)*, 887.
(238) Ozin, G. *Adv. Mater.* **1992**, *4 (10)*, 612.
(239) Novak, B. M.; Auerbach, D.; Verrier, C. *Chem. Mater.* **1994**, *6 (3)*, 282.
(240) Osada, Y.; Ross-Murphy, S. B. *Scientific American* **1993**, *May*, 82.
(241) Shibayama, M.; Tanaka, T. *Adv. Polym. Sci.* **1993**, *109*, 1.
(242) See, for instance, Smart Gels from Gel Sciences, Bedford, MA.
(243) Dagani, R. *Chem. Eng. News* **1997**, *75 (23)*, 26.

CR9700282